Solar Energy 203 (2020) 46–68

Contents lists available at ScienceDirect

Solar Energy

journal homepage: www.elsevier.com/locate/solener

An analytical indoor experimental study on the effect of soiling on PV, focusing on dust properties and PV surface material

Yusuf N. Chanchangi*, Aritra Ghosh, Senthilarasu Sundaram, Tapas K. Mallick

Environment and Sustainability Institute (ESI), University of Exeter, Penryn Campus TR10 9FE, United Kingdom

ARTICLE INFO

Keywords:
Soiling
Dust properties
PV surface material
PV performance

ABSTRACT

Photovoltaic technology penetration is experiencing noticeable progress. However, its performance is significantly affected by soiling, which is influenced by several factors such as site characteristics, weather, tilt angle and surface orientation, surface material and dust properties. This indoor study investigates the effect of soiling on photovoltaic modules, focusing on dust properties and PV surface materials as influencing factors. A Solar simulator, spectrometer and SEM/ EDX were used to characterise and investigate the effect of accumulation of 13 different samples (ash, bird droppings, carpet dust, cement, charcoal, clay, coarse sand, laterite, loam soil, salt, sandy soil, stone dust and wood dust) on PV performance. The findings develop upon previous studies on the effects of dust particle accumulation on PV performance by using more dust samples and applying more rigorous techniques. The results show that charcoal appears to have the worst degradation effect on PV performance with about 98% reduction in short circuit current while salt seems to have the least impact with about 7%. The influence of 2 PV surface materials (acrylic plastic and low iron glass) on dust accumulation were examined, and results show that the acrylic plastic accumulates more dust when compared to low iron glass. Results also show that dry deposition has a reduced adhesion to the coupons compared to wet deposition. The findings could be used in selecting PV farm sites by avoiding areas with high pollution, and it could stimulate further research on selecting an appropriate mitigation technique. The ramifications caused because of soiling cannot be overlooked or overemphasis; as such there is a need to identify appropriate and cost-effective mitigation techniques that can continue to promote the global penetration of PV technologies and sustain its performance.

1. Introduction

By exploiting free, natural abundant solar radiation, solar photovoltaic (PV) technology is becoming the most promising clean energy harvesting system and the fastest growing renewable energy technology due to a remarkable decline in price and zero noise during operation (Hammad et al., 2018). However, this technology is facing a severe challenge during its operation, due to the effect of dust formation that degrades its operational performance (Costa et al., 2018). Factors such as local environment, weather conditions, tilt angle and surface orientation, surface material and dust properties can influence dust deposition on the PV system (Mani and Pillai, 2010; Kaldellis and Kapsali, 2011).

Shape, size, roughness and weight of particles can influence the extent to which light transmission is reduced. The diameter of dust grain includes fine-grain which is $<$ 0.05 mm (predominantly clay and silt size), medium-grain which is 0.05–2 mm (mostly sand size) and coarse grain, which can vary between 2 and 57 mm (mainly gravel) (Al-Shabaan et al., 2016; Picotti et al., 2018). The roughness of a dust particle can be fine or coarse. Fine dust particles have a higher tendency adhesion than coarse dust particles, allowing them to be distributed uniformly over a PV surface causing higher light scattering and lower transmission (Tanesab et al., 2015). In addition, a porous layer allows more light transmittance than a smooth layer (Nirmal et al., 2014). Non-spherical and coarse particles have more potential to cause scattering than a spherical particle with a fine surface (Li et al., 2004). Diagonal or hexagonal particles have higher single scattering albedo when compared to dust particles with spheroid and ellipsoidal structures (Mishra et al., 2015). In contrast, Potenza et al. (2016) reported a finding that strongly conflicts with the findings of other studies that, non-spherical dust particles account for higher transmissivity when compared to spherical. Tanesab et al. (2019) supported this claim and stated that dust structures that appear to have angular and diagonal structures have better optical properties than spheroids or elliptical

* Corresponding author.
E-mail addresses: yc486@exeter.ac.uk (Y.N. Chanchangi), t.k.mallick@exeter.ac.uk (T.K. Mallick).

https://doi.org/10.1016/j.solener.2020.03.089
Received 21 December 2019; Received in revised form 13 March 2020; Accepted 23 March 2020

Nomenclature

(λ)	Relative spectral distribution of solar radiation
T (λ)	Spectral transmission
Δλ	Change in wavelength
φ	PV electrical output parameters
SL_{PV}	PV soiling
I_{sc}	Short circuit current (A)
V_{oc}	Open circuit voltage (V)
FF	Fill factor
I_{max}	Load current which maximises the output power
V_{max}	Voltage that maximises the power output
P_{max}	Maximum power output of a module
$P_{max,clean}$	Maximum power output of a clean module
$P_{max,dusty}$	Maximum power output of a dusty module
R	Radius
surf	Particle surface
A	Cross-sectional area of dust particle
Lproj	Longest length of dust particle
P	Perimeter of dust particle.
γ	Gamma - Surface tension of water
ζ	Distance between flat surface and particle
ι	iota- Separation distance
θ	Theta – contact angle
p	Density
ε	Epsilon - Dielectric constant
εo	Epsilon naught - Permittivity of free space
A	Hamaker constant

structures. Smaller dust particles have a stronger adhesion force and a greater negative impact than larger particles since they occupy smaller spaces and attenuate light, whereas larger particles leave porous spaces where light can penetrate. Also, smaller dust particles have a stronger adhesion force than the lift force generated by wind and sometimes even stronger than the lift force generated by rain which limits the cleaning capacity of rainfall when compared with large dust particles (Abderrezek and Fathi, 2017). A deposited dust particle with a greater mass reduces the voltage, ampere and power more than a dust particle of lower mass (Kazem and Chaichan, 2016).

Characterisation of manual dust deposition on PV surface has previously been performed within an indoor laboratory environment. The impact of the physical properties of six different types of dust collected from North Oman showed about 30% − 40% degradation of power output and that dust samples with the highest moisture content, specific gravity and plasticity index caused greatest deterioration of PV performance (Kazem and Chaichan, 2016). An investigation into the effects of ash, sand, calcium carbonate, red soil and silica on the performance of a polycrystalline PV module showed ash accounted for about 25% of PV voltage reduction and has a greater negative effect in comparison to other samples (Kazem et al., 2013). Power output due to carbon, cement and three classes of limestone deposition showed that finer dust particles could cause more PV performance degradation than coarse dust particles (El-Shobokshy and Hussein, 1993). Performance degradation of PV due to fly ash, limestone and red soil showed that red soil accounts for the highest reduction in PV performance followed by limestone and fly ash (Kaldellis et al., 2011). Sulaiman et al. (2011) investigated the effect of dust on PV performance using mud and talcum samples. The results showed a reduction in peak power output of about 18% with 6% difference between the two samples. Wang et al. (2020a) reported high PV yield degradation. The researchers showed that the maximum power of a clean PV module degraded to about 82.1% from the original power after exposure while a module that was earlier dirty and cleaned before testing degraded to about 46.7%. This shows that if a dirty module is subsequently cleaned, it becomes more prone to dust accumulation. Alnasser et al. (2020) examined the effect of dust accumulation on PV performance. Researchers showed that 100g/m^2 of sand, ordinary cement, egg cement, gypsum, or industrial gypsum, caused 12%, 14%, 15%, 9% and 10% PV yield reductions respectively. Adıgüzel et al. (2019) investigated the effect of coal on light transmittance and reported 62.05% degradation of PV performance when 15g of tiny particles (38 μm) of coal were examined and 28.90% degradation when larger particles (250–500 μm) were used.

Desert areas are recognised as primary sources of dust as reported by Ilse et al. (2018) and are associated with airborne dust containing mineral compositions such as carbonates, feldspar, gypsum, illite, iron oxides, kaolinite, quartz and smectite. Ilse et al. (2018) reported that the mineral composition of dust has a strong influence on the optical/transmittance behaviour when deposited on a coupon. Sarver et al. (2013) stated that mineral composition is a vital element to adhesion processes, especially when capillary force is activated.

In this study, density is divided into two aspects; deposition density (the degree of deposition) and density of the minerals, and for this research, literature related to both were reviewed. The current study focuses on the role of mineral density on dust formation and its effect on PV performance, which is not adequately reported in the literature. Since samples were artificially deposited, and it will be a challenge or nearly impossible to determine the average deposition density of various locations across the world.

Zaihidee et al. (2016) reported that the degree of PV performance degradation depends on dust deposition density. They further provide a result that shows a decrease of PV performance where short circuit current degrades by about 15–21%, open-circuit voltage by 2–6% and the efficiency by 15–35% when 20 g/m^2 was deposited. Klugmann-Radziemska (2015) researched dust thickness and reported that dust thickness on PV is linear to PV efficiency decrease when it is less than 3 μm. Tanesab et al. (2019) confirm the effect of dust deposition density in a study which showed a linear decrease in light transmittance when PV surfaces were deposited with two types of dust which had densities of < 0.3 mg/cm^2.

Several review papers providing comprehensive information were reported in the following synopsis: Darwish et al. (2015) provided critical and challenging review questions to be used in analysing the effect of dust type pollutant on PV performance. Sarver et al. (2013) provided a comprehensive review on the impact of soiling on PV focusing transmittance and surface reflectance associated with sand as a dust sample and its moisture content in various locations with high solar potential around the world. Sayyah et al. (2014) provided a review of studies that reported energy yield loses of PV plants and laboratory studies so that PV farm designers can have a database on predicting foiling losses and assessing effective mitigation techniques. Zaihidee et al. (2016) described the effect of dust formation on PV performance and summarised the impact of influencing factors such as weather, dust property, PV installation and PV module type. Costa et al. (2018) provided a review containing a comprehensive catalogue of solar PV, concentrating solar thermal power publications as a guide for readers and researchers. Figgis et al. (2017) provided a review of dust particle mechanics related to desert conditions for identification of mitigation techniques. Gupta et al. (2019) provided a review on factors causing dust deposition on PV surfaces and their impact on the optical, thermal and electrical characteristic of the solar PV module. This review also summarised the different mitigation techniques, which can help in selecting an appropriate method for removing dust. Chanchangi et al. (2020) provided a review on the effect of dust accumulation on PV performance in Nigeria, discussing various factors influencing dust accumulation. The authors also highlighted various mitigation techniques and recommended further research on investigating the optimisation of the most suitable method to either reduce or prevent dust accumulation

on PV.

Influencing factors on PV soiling, such as dust properties, have been investigated by a number of researchers, as reported earlier in this section but, only a few dust samples were examined. This study investigated a significantly larger number of dust samples and considered other parameters such as comprehensive investigation and analysis of both morphological and chemical/mineral composition that were overlooked or not adequately considered in previous work. The most commonly used PV surface materials (acrylic plastic and low iron glass) were among the parameters investigated. This report contributes to the body of knowledge in the field of soiling on PV and can serve as a guide to engineers for selecting solar farm sites and also to plan for adequate mitigation techniques. This work highlights the significance of soiling issues and provides a useful foundation that can stimulate further research on mitigation approaches. The next section describes the dust samples, coupons and procedures used in this research. Part 4 is a detailed presentation of results. Part 5 is a discussion of these results.

2. Method

Zaihidee et al. (2016) stated that conducting an indoor experiment includes the comfort of selecting an appropriate dust sample to be used. For this research, 13 dust samples were collected from Nigeria, measured and quantified, Fig. 1 is the digital image showing all the samples. Each sample was loaded into a 40 ml bottle and weighed using ME204 Mettler Toledo sensitive digital scale. The weight of each sample is documented in Table 1 below. Each sample was deposited using two approaches (dry and wet) on two different materials (low iron glass and Acrylic plastic). The materials were selected because of their high-level transmittance properties, and they are widely accepted and used materials in the PV industry. Each piece of low iron glass and acrylic plastic had a dimension of 13 × 13 × 0.4 cm. A mini-module with an active area of 120.84 cm^2 was developed using four monocrystalline cells with dimensions 5.2 cm × 5.2 cm.

These weights mentioned in Table 1 are the initial average used for both depositions. All samples are dry except bird droppings, which had particles in semi-solid form. It was observed that tipping of the coupons and wind effects also caused blowing off, rolling and sliding of particles. Particle weight was not measured after deposition; therefore, the exact weight of deposited particles that remained on the coupons was not measured. In addition, the wet deposition might have additional weight since water was used, and the weight was not measured.

Table 1
Dust samples.

Sample	Weight
Ash	21.8 g
Bird droppings	16.2 g
Carpet dust	10.3 g
Cement	33.2 g
Charcoal	15.6 g
Salt	48.1 g
Sand - Coarse	54.4 g
Sand - Laterite	41.0 g
Soil - Clay	44.3 g
Soil - Loamy	50.9 g
Soil - Sandy	40.3 g
Stone dust	46.5 g
Wood dust	10.3 g

2.1. Samples preparation and deposition

Determining an appropriate way to simulate the dust deposition for an indoor experiment is a critical task. Injection and fan mixing (Jiang et al., 2011), spraying sample with water content (Kaldellis et al., 2011), using a wind tunnel and manually discharging samples from a dust cloud producer (Goossens and Van Kerschaever, 1999), using a diffuser integrated with a sandblaster (Al-Hasan, 1998) and by manual sieving and free fall from a tube (Beattie et al., 2012; Qasem et al., 2011) are the reported methods for this work. All these methods resulted in different cluttering patterns and uniformity on the platform. However, natural dust depositions are not the same around the world. This research adopted the manual and free-fall approach as reported by Beattie et al. (2012) and Qasem et al. (2011) based on its simplicity to achieve natural positioning, initial bouncing and resuspension of particles that occurred in the natural deposition. However, this approach does not give the accurate representation of natural dust accumulation, but it permits experimenting with extreme soiling conditions to highlight degradation that could occur during extreme weather such as a sand storm, volcanic eruption, wildfire, tornado, hurricane, storm and other natural disasters.

Fig. 1. Digital images of dust samples.

Samples were deposited using an in-house developed dispenser, which was made using a 3D printer with thermoplastic Polyurethane. The dispenser was designed to only allow particles less than or equal to 2 mm to fall. The dispenser was initially used to sieve samples to eliminate particles > 2 mm. It was later used to spread out a bottle (40 ml) of each sample on each of the coupons (low iron glass or acrylic plastic). The inertial force was applied by the design of the dispenser where the upper part has a wider opening, and the lower part is narrowed down to only allow particles less than or equal to 2 mm to pass through, enabling Brownian diffusion to take place where particles collide with one another to settle on a coupon. Particles become adhered to one another due to Van der Waals forces that make small dry particles adhere to one another. Samples were deposited and allowed to settle for about 24hrs to promote sedimentation. Then the coupons were tilted to about 45° to allow the gravitational effect to remove particles that have not adhered to the coupon. In addition, coupons were tilted to about 90°, and subsequently exposed to a table fan which generated wind at a velocity of 4 m/s to simulate wind effect (see Fig. 2 for dry deposited samples). This approach is used to represent the dry season dust deposition. Said and Walwil (2014) stated that water exists between the dust particles, creating capillary bridges both between the particles dust and between particles and the surface. It has been reported by Isaifan et al. (2019) that, capillary forces proliferate when the relative humidity is above 70%. Natural relative humidity and dew were avoided in order to avoid biasing the parameters.

The wet deposition is used to represent the dew and rainy season dust deposition. The same dispenser was used in spreading the same amount of dust on the surface area of the coupons. This time, coupons were sprayed with about 20 ml of water before and 20 ml after deposition of dust samples and were allowed to dry for up to about 24hrs. This amount was the same quantity that made each sample become 100% saturated with water and promoted capillary forces. The initial 20 ml water spray was to simulate dew while the spraying after deposition was to simulate light rainfall so that diffusiopherisis will allow cementation of particles considering the capillary bridges that were created by the water (see Fig. 3 for wet deposited samples). Coupons were tilted to about 45° and 90° to allow gravitational effects and exposed to a table fan which generated wind at a velocity of 14 km/hr (~4m/s). This wind velocity used in this study falls within the ranges of wind speed in Nigeria. Argungu et al. (2019) reported that, average wind speed at the height 10 m in northern ranges from 4.0 to 5.12 m/s and 1.4–3.0 m/s in the southern part. Blowing of wind towards the coupon is an attempt to remove some particles using a natural mitigation approach. Kazem and Chaichan (2019) stated that whenever the wind direction faces a PV module's surface, the air movement removes a certain amount of dust particles that have accumulated. Gholami et al. (2017) stated that the critical levels that determine the dust accumulation on the PV module are average wind speed above 4 m/s and relative humidity below 50%.

Several attempts were made to acquire natural bird droppings deposition by placing coupons in strategic locations where birds were usually found but was not achieve. Bird droppings were collected in semi-solid and solid forms and were preserved in bottles to maintain freshness. During both depositions, samples were poured over the coupon surfaces without using the dispenser.

2.2. Procedure

2.2.1. Spectral test

The optical characterisation was conducted to determine transmittance deterioration level caused by each dust sample on various coupons using the Perkin Elmer Lambda 1050 UV/VIS/NIR spectrometer. Clean low iron glass and acrylic plastics were first tested to identify and confirm the actual transmittance levels of the coupons. Each sample from the various deposition methods was then subjected to spectral transmittance evaluation. UV (Ultraviolet), VIS (Visual) and NIR (Near Infra-Red) transmittance level of each sample was measured, ranging 250 nm to 1250 nm wavelength. This is to investigate the transparency of the dust samples considering the wavelength within which the used PV technology (monocrystalline solar cells) responds, as mentioned earlier. The transmittance results are validated using the following Eq. (1).

$$\tau_{solar} = \frac{\sum_{\lambda=300nm}^{1250nm} S(\lambda)T(\lambda)\Delta\lambda}{\sum_{\lambda=300nm}^{1250nm} S(\lambda)\Delta\lambda}. \quad (1)$$

where S (λ) is the relative spectral distribution of solar radiation, T (λ) is the spectral transmission, and Δλ is the change in wavelength.

The schematic diagram of the spectrometer is provided below in Fig. 4 to illustrate how the transmittance was measured.

2.2.2. Image analysis

Image characterisation was conducted to determine the morphology and chemical composition of each dust sample. Samples were carbon prepared using Em-Tec low profile pin stub with a diameter of 25 mm and a conductive carbon tab. Samples were carbon-coated using the Emi-Tech K950 carbon coating machine before they were subjected to image scanning using the SEM (S) Quanta FEG 650, which was equipped with an EDX (Energy Dispersive X-ray). The morphology of each sample was characterised using the shape and size of the backscattered electrons (BSE) and the secondary electron (SE) imaging. The chemical composition of each sample was identified using the EDX results and further analysed using specific information such as diaphaneity and mineral density from online mineralogy databases such as

Fig. 2. Dry deposition.

Fig. 3. Wet deposition.

webmineral.com, mindat.org and minerals.net. Surface roughness was observed and analysed by comparing SEM images obtained in this research and SEM images reported in the literature mentioned above.

Size and shape of the particle were analysed using SEM images and equations provided in the literature. The surface diameter and area were measured and estimated from the SEM images. Aïssa et al. (2016) provided equations (Eqs. (2) and (3)) which were adopted for analysing the SEM images using the aspect ratio and particle shape. Shapes were determined using SEM images that present a 3D view of the dust particle.

$$(Aspectratio) = \frac{\pi (L_{proj})^2}{4A}. \quad (2)$$

where A is the cross-sectional area of the dust particle, $Lproj$ is the longest length of the dust particle.

$$(shape) = \frac{P^2}{4\pi A}. \quad (3)$$

where P is the perimeter of the dust particle.

Kalashnikov and Sokolik (2004) also provided an equation (Eq. (4)) to estimate the surface radius. This research adopted the equation since all parameters can be measured and estimated, and it was achieved using Eq. (4) and the estimated dimensions obtained from the SEM images. All estimations were presented in Table 2.

Table 2
Mini module's parameters.

Parameter	**Value**		
Type	Monocrystalline solar module		
Surface material	Clear	Acrylic plastic	Low iron glass
Maximum power (Pmax)	1.62 W	1.55 W	1.5 W
Output tolerance	0 ~ ± 5%		
Maximum voltage (Vmpp)	2.0 V	2.0 V	2.0 V
Maximum current (Impp)	0.82A	0.77A	0.76A
Open circuit voltage (Voc)	2.5 V	2.45 V	2.44 V
Short circuit current (Isc)	0.95A	0.90A	0.89A
Weight	229.4 g	310.0 g	392.6 g
Fill factor	0.7	0.704	0.703
Dimensions	150 mm × 150 mm		
Dimensions (active area)	11 mm × 11 mm		
Test conditions	1000 W/m^2, AM 1.5, T = 25 °C		

$$R_{surf} = \sqrt{S}/4\pi. \quad (4)$$

where R is the radius and surf is the surface of the particle. Fig. 5 illustrates the image characterisation procedure conducted on each of the samples.

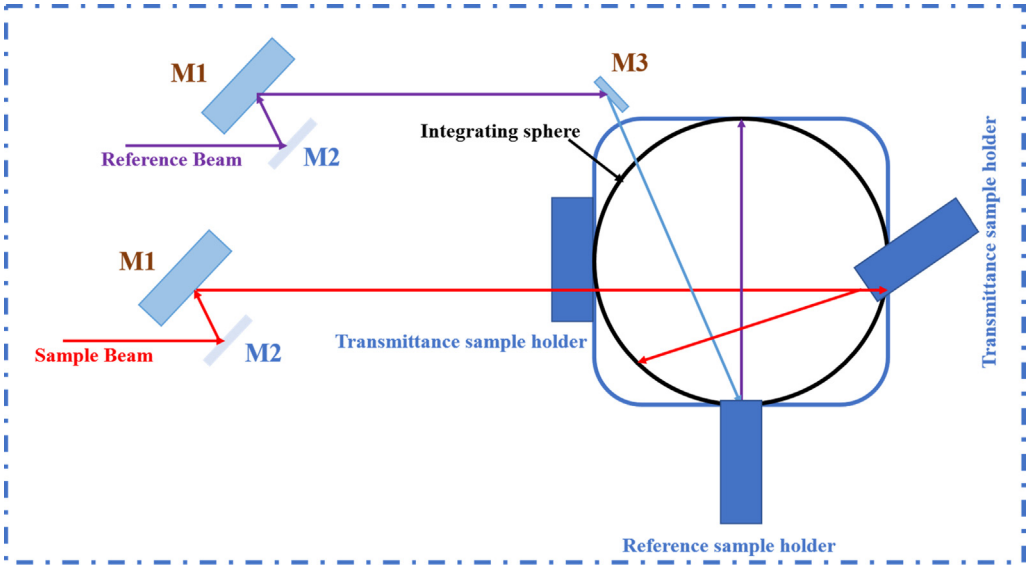

Fig. 4. Schematic diagram of Perkin Elmer® Lambda 1050 UV/VIS/NIR spectrometer illustrating the transmittance test procedure.

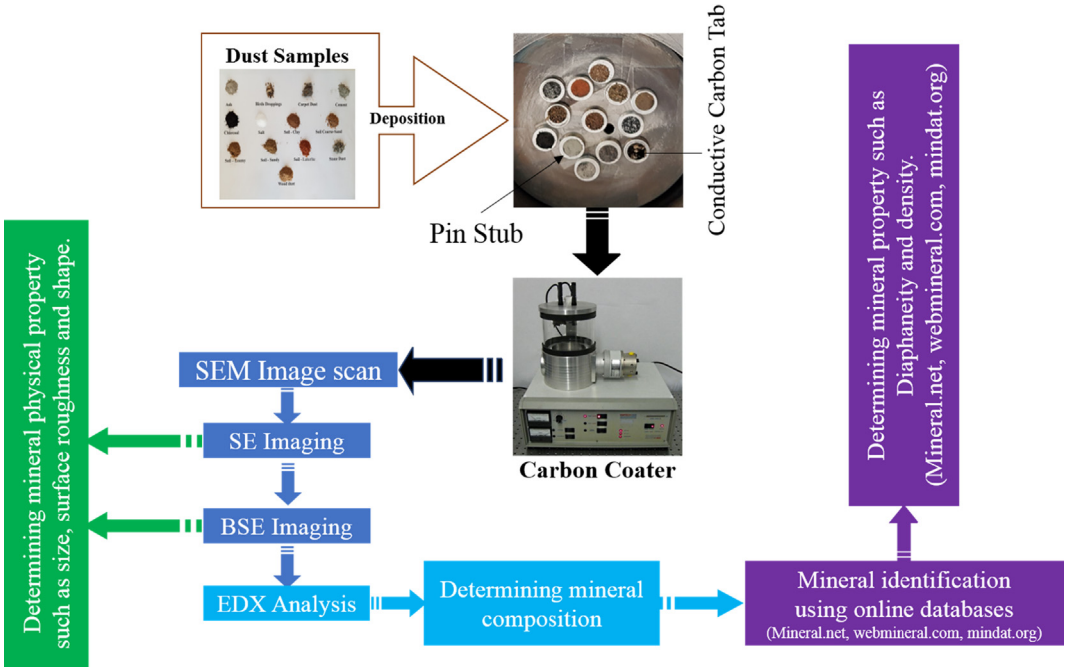

Fig. 5. Image characterisation.

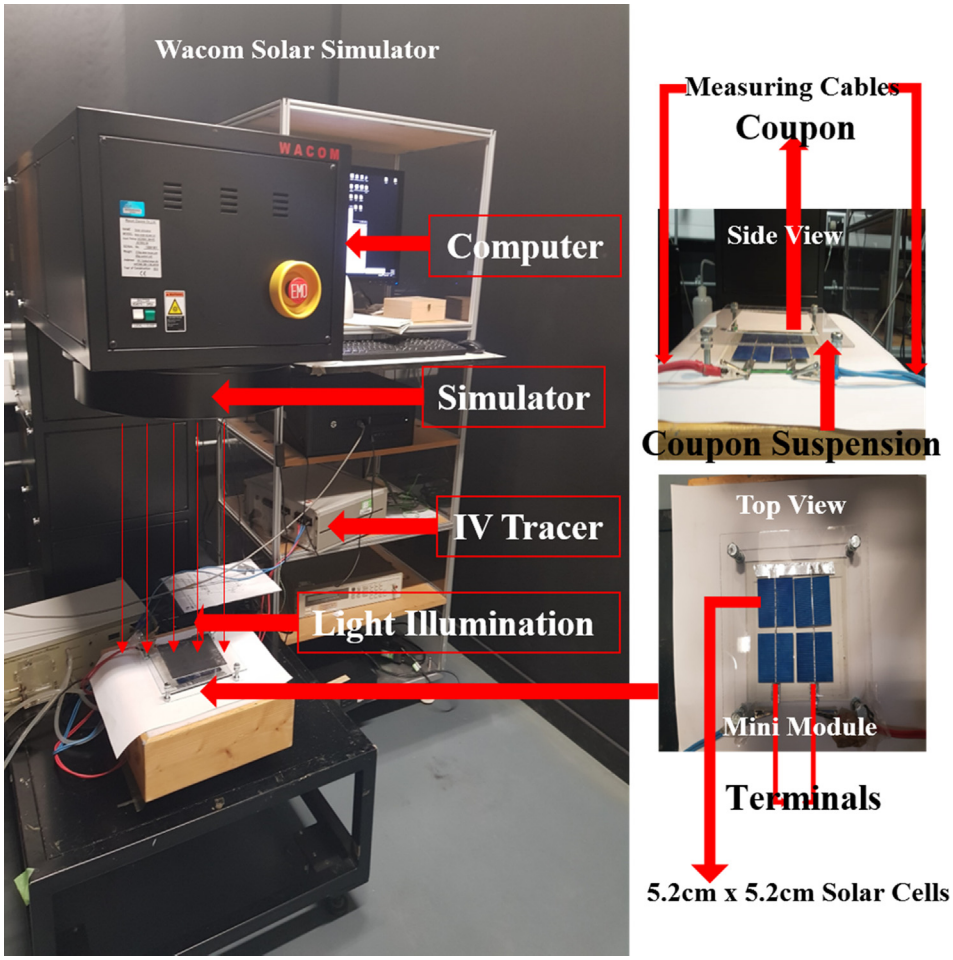

Fig. 6. Solar simulator procedure.

2.2.3. PV performance measurement

The mini module's performance was tested using a Wacom continuous solar simulator at a controlled temperature of 25 °C and was subjected to several tests using thirteen dust samples deposited on the two types of coupons, as mentioned in Section 2.1. The module was initially tested without surface covering to obtain baseline performance data of the module. Then modules were individually tested with a covering of clean acrylic plastic and low iron glass coupon. The device was further tested by covering the active area with each of the dust samples from the two deposition methods highlighted above. Current and voltage data were generated, and the power data were computed to plot the I-V/P-V (current – voltage/power – voltage) curves for analysis. The effect of air vacuum between the solar cells and the coupons used was ignored since the experiment was focusing on the reduction in short circuit currents and therefore, modules were not exposed to light for an extended period to avoid temperature excitement that can lead to voltage degradation, which in turn could affect the overall output of the device. Thermophoresis was prevented during the experiment since the ambient temperature and the PV temperature are equal throughout the period. The results obtained allow easy data analysis and highlight the power degradation caused by the various dust samples deposited on the different surface materials. A schematic diagram representing the procedure of PV performance measurement is illustrated in Fig. 6 below.

To validate the results, mathematical equations provided by Hachicha et al. (2019) and Kalogirou (2009) were adopted. Eq. (5) was used in determining the degradation of PV performance caused by dust accumulation using normalised electrical PV characteristics such as voltage, current and power.

$$\varphi \text{ normalised} = \frac{\varphi \text{ dusty}}{\varphi \text{ clean}} \tag{5}$$

where φ represents the PV electrical output parameters (voltage, current and power), this is further validated using soiling Eq. (6) which is relative to a clean surface.

$$SL_{PV} = \frac{P_{max,clean} - P_{max,dusty}}{P_{max,clean}} / P_{max,clean} \tag{6}$$

where SL_{PV} is PV soiling, P_{max} is maximum power which passes through the maximum power point when the load resistance is optimum, and the dissipated power to the resistive load is maximum, $P_{max,clean}$ represents the maximum power output of a clean module and $P_{max,dusty}$ represents a module with dust accumulation.

$$P_{max} = I_{max} V_{max} \tag{7}$$

where I_{max} is the load current which maximises the output power, and V_{max} is the voltage that maximises the power output, and P_{max} can be represented using equation (8):

$$P_{max} = I_{sc} V_{oc} FF \tag{8}$$

where I_{sc} is the short circuit current, V_{oc} open-circuit voltage and FF is the fill factor obtained from the IV tracer. The FF can be calculated using Eq. (9).

$$FF = \frac{P_{max}}{I_{sc} V_{OC}} = \frac{I_{max} V_{max}}{I_{SC} V_{OC}} \tag{9}$$

3. Results and analysis

This section presents the results of all the experiments mentioned above. PV performance results, spectral results and SEM images of each dust type are presented to describe the effect of the individual sample. The mini module's IV/PV (current and voltage/power and voltage)

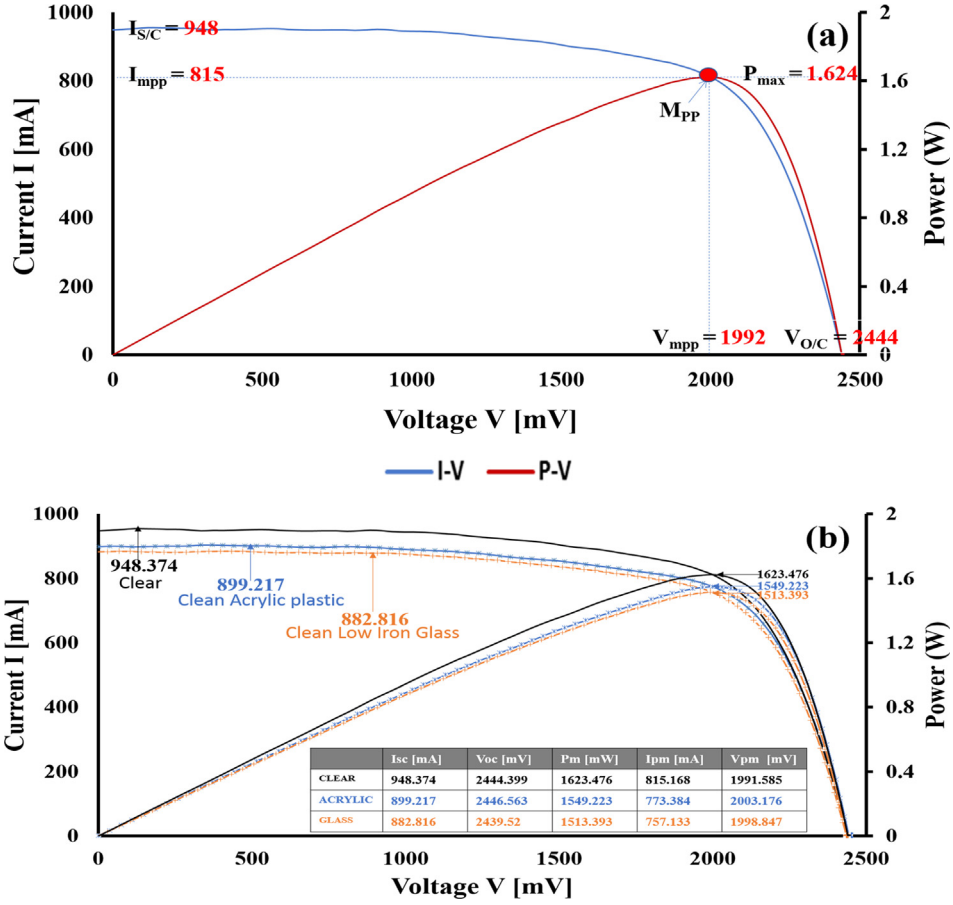

	Isc [mA]	Voc [mV]	Pm [mW]	Ipm [mA]	Vpm [mV]
CLEAR	948.374	2444.399	1623.476	815.168	1991.585
ACRYLIC	899.217	2446.563	1549.223	773.384	2003.176
GLASS	882.816	2439.52	1513.393	757.133	1998.847

Fig. 7. Mini module's IV/PV curve (a) clear, (b) clear, clean acrylic plastic and clean glass.

curve is initially introduced in Fig. 7 to show the optimum performance of the system and its IV and PV characteristics.

3.1. Ash

The sample ash is also known as fly ash and is a fine by-product of burnt dry wood, which is a common source of dust in developing countries due to the use of farm by-products to generate energy. Combustion of materials such as wood in high temperatures leads to the production of both fly and bottom ash. The fly ash can be transported by wind. Results from the various experiments show that when ash is considered as a source of dust, it has a detrimental effect on the PV performance because it obstructs the photovoltaic effect from reaching the solar cells of a PV module (Kazem et al., 2013; Kaldellis et al., 2011) and Fig. 8 confirms this assertion.

Fig. 8 shows the spectral transmission, SEM and PV performance while coupons (acrylic plastic and glass) were deposited with ash. Light transmission reduction was recorded when ash was dry deposited on coupons with levels of 55% reduction for acrylic and 4% for low iron glass. On the other hand, very high reduction of transmittance was recorded when it was wet deposited, where acrylic plastic had 99%, and low iron glass has 87% degradation. The image characterisation shows that ash dust particles appear to have minerals that seem to be opaque, angular in structure, small in size (μm), dense and have a coarse surface. The short circuit current (I_{sc}) degraded by about 56% when ash was dry deposited on acrylic plastic and about 22% on the low iron glass. It also shows that about 94% of Isc degraded when the ash sample was wet deposited on the acrylic plastic and similarly on the low iron glass.

3.2. Bird droppings

This is the faeces of flying birds, which is a combination of liquid and semi-solid materials. Faeces comprise a mixture of three components, depending on the bird's consumption; uric acid, which comes in the liquid form, the green material and whitish parts which are semi-solid. These materials are always opaque. Bird droppings have a devastating effect on light transmittance, which can reduce the Pmax (maximum power) of a module. The results below highlight the effect of soiling caused by bird droppings on PV performance.

Fig. 9 shows the spectral transmission, SEM and PV performance when coupons (acrylic plastic and glass) were deposited with bird droppings. Very high transmission reduction was recorded when bird droppings were deposited onto coupons with acrylic reaching 90% and low iron glass 54%. On the other hand, when the bird droppings were wet deposited, a reduction of about 87% was recorded on acrylic plastic and of 75% on the low iron glass. Image characterisation shows that bird droppings comprising many different minerals appear to be transparent, translucent, and opaque, which reduces the penetration of light. Density of the materials observed would slow flux intensity and can cause light absorbance. The surface of the particle was found to be fine and smooth, which promotes light scattering. Sample shape appears to be aggregated, and the sizes were not uniformly distributed because some parts appeared to be large while others were tiny. Light can penetrate through the areas with larger particle deposition because they are porous. In addition, due to lack of a urinary bladder, bird droppings come with a percentage of liquid (uric acid), and this promotes capillary bridges that can lead to the closure of small gaps and porous areas, which disrupt light penetration and further promote cementation. The PV performance results show that the short circuit current degraded by about 46% when bird droppings were deposited on the acrylic plastic and about 35% on the low iron glass. In addition,

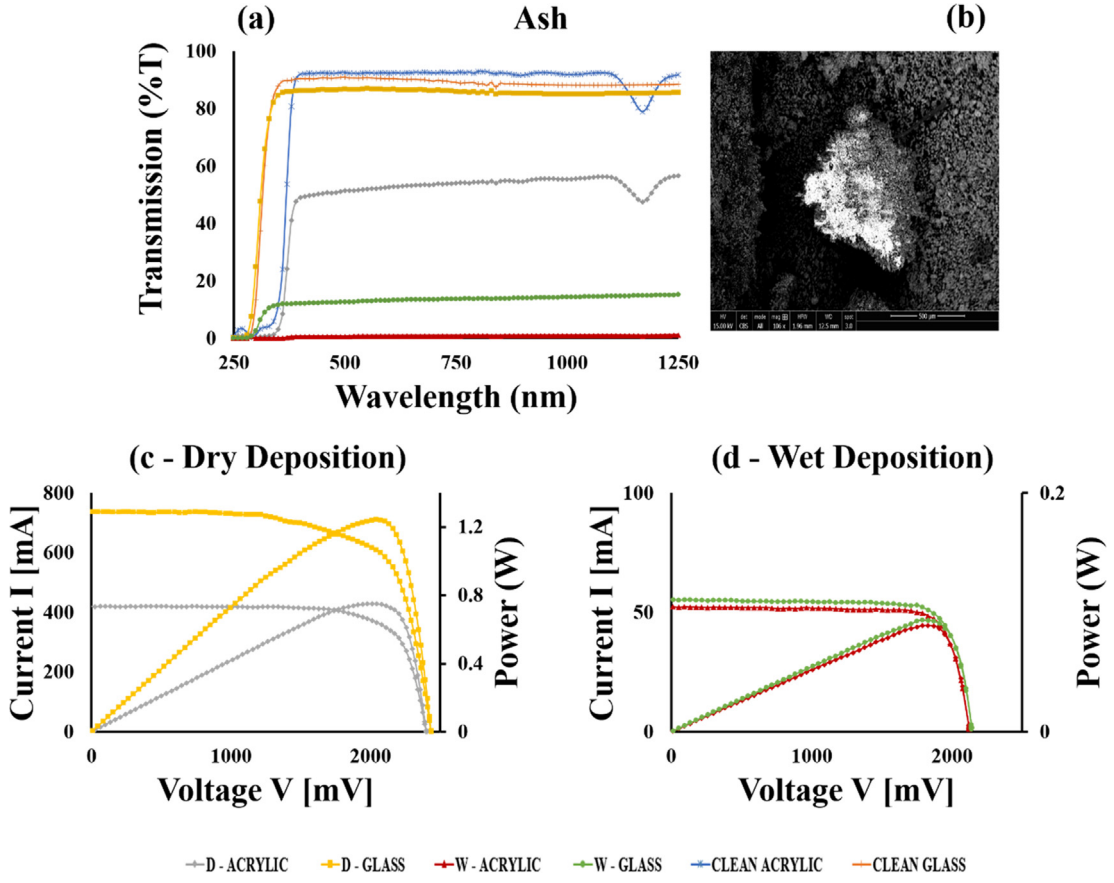

Fig. 8. Ash - (a) Spectral transmittance (b) SEM imaging (c and d) PV performance.

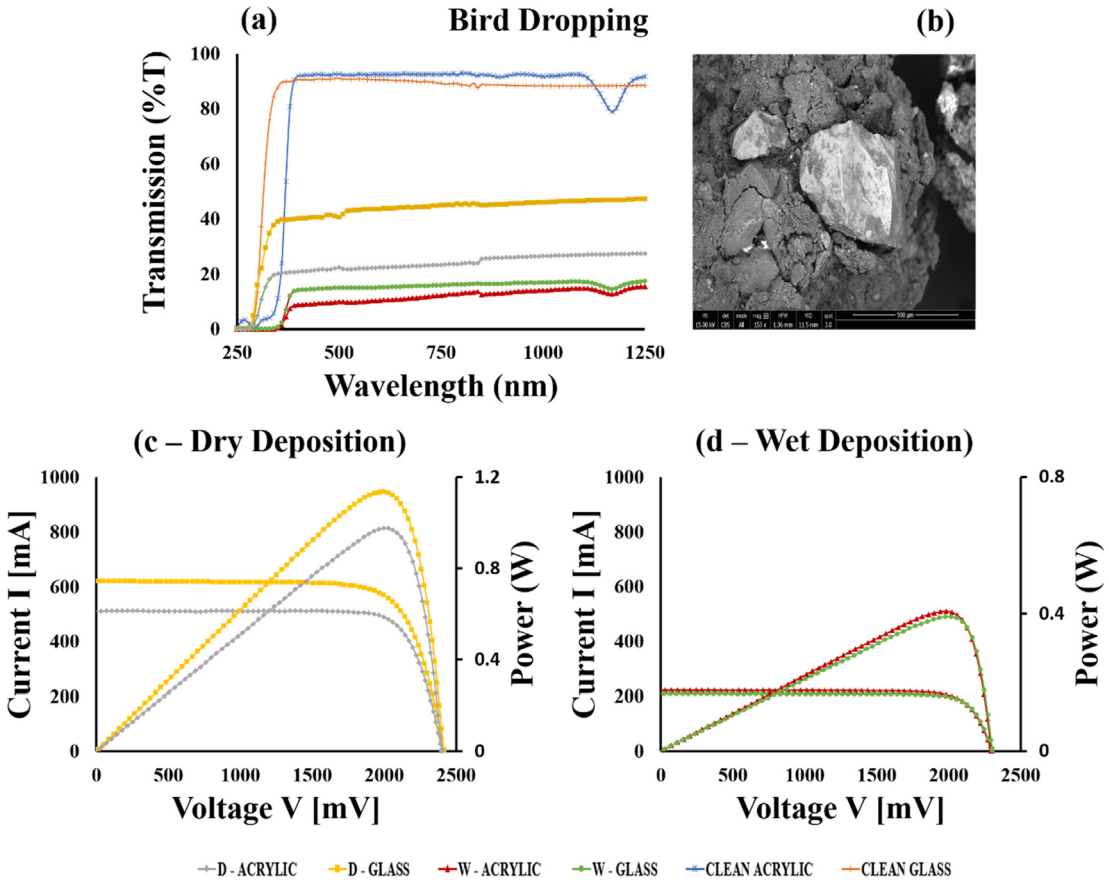

Fig. 9. Bird droppings - (a) Spectral transmittance (b) SEM imaging (c and d) PV performance.

further degradation was observed when more water was added to various coupons to simulate light rain and dew. An almost two-fold deterioration was observed, with about an 87% reduction in the short circuit current when deposited on the acrylic plastic and 74% reduction when deposited on the low iron glass.

3.3. Carpet dust

These are particles stored in carpets, and some are visible while others are not. These particles can be anything, including volatile organic compounds. According to Becher et al. (2018), carpets are the repository for indoor air pollutants such as dust particles, biological contaminants, dirt and allergens. Some of these materials can be emitted into the air and transported by the wind in the atmosphere and when deposited on a PV module can cause light transmittance disturbances. The results below highlight the effect of soiling due to carpet dust on PV performance.

Fig. 10 illustrates the spectral transmission, SEM and PV performance when coupons (acrylic plastic and glass) were deposited with carpet dust. Meagre light transmission reduction was recorded when carpet dust was dry deposited on the coupons with acrylic plastic showing about 8% and low iron glass just 1% reduction. On the other hand, high reduction was recorded when carpet dust was wet deposited on coupons where almost 100% decrease was documented on both coupons. Image characterisation shows that carpet dust combines a wide range of minerals, and the sample used for this research appears to be translucent and opaque, which can attenuate light transmittance. Minerals appeared to have a high mineral density, which can slow down the flux intensity of light. The surface of the particles was observed to be coarse and might possess good light transmittance qualities. Particle sizes appear to be a combination of tiny invisible and large visible particles, but all particles were very light in weight. Sample shape appears to be a bent angular/triangular channel-like structure, which represents a better optical property and can promote light penetration. Even though the carpet dust possesses some positive light transmittance qualities, the negative qualities surmount. The PV performance result shows that the short circuit current degraded by about 9% when carpet dust was dry deposited on the acrylic plastic and 7% on the low iron glass. An alarming increase was observed when the sample was wet deposited on the various coupons where degradation of about 91% on the acrylic plastic and 92% on the low iron were recorded.

3.4. Cement

This is a fine complex mixture of several compounds composed using high temperatures of > 1400 °C and is used as building material (Taylor, 1992). Various types of compounds are used in producing cement; the chemical components of each cement type depend on the company. Cement is light in weight and can be transported by the wind in the atmosphere from one location to another. Moreover, when deposited on a PV, it can reduce or obstruct light transmittance. The results below highlight the effect of soiling caused by cement on PV performance.

Fig. 11 illustrates the spectral transmission, SEM and PV performance when coupons (acrylic plastic and glass) were deposited with cement. When cement was dry deposited on coupons, light transmission was reduced by about 34% on acrylic plastic and 4% on the low iron glass. On the other hand, the high reduction was recorded when cement was wet deposited on coupons with acrylic plastic recording about 95% and low iron glass about 99% reduction. The image characterisation shows that cement particles appear to be opaque with the capacity of attenuating light. These minerals appear to have high density, which can slow the flux intensity of light resulting in light absorbance. Particle surfaces are coarse, which present good quality of light transmittance.

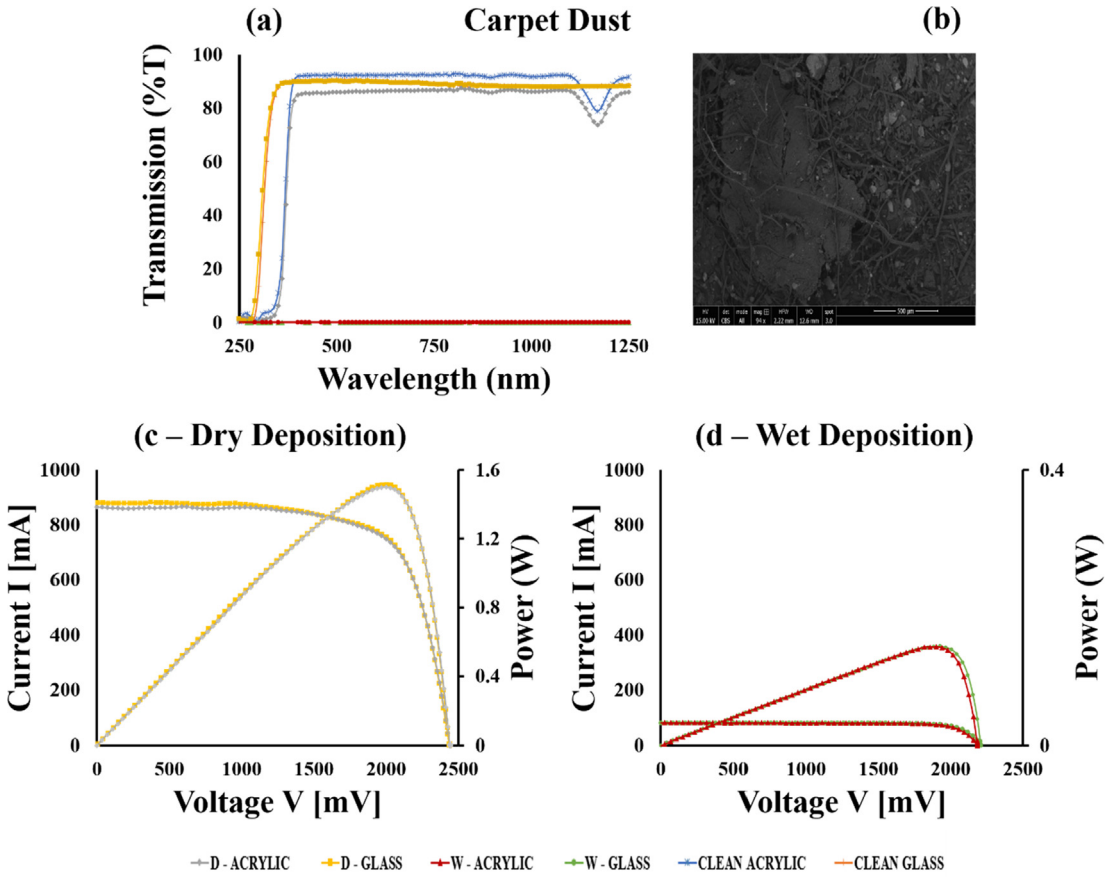

Fig. 10. Carpet dust - (a) Spectral transmittance (b) SEM imaging (c and d) PV performance.

The particles are tiny in size, and this can attenuate the light. An angular flattened shape was observed, which promotes the optical property of minerals and allows more transmittance of light. Even though the sample has some good optical qualities, the negative qualities surmount. The PV performance result shows that the short circuit current degraded by about 21% when cement was dry deposited on acrylic plastic and 8% on the low iron glass. The high increase in degradation was observed when the cement sample was wet deposited on the various coupons where degradation of about 94% on acrylic plastic and 96% on low iron glass were recorded.

3.5. Charcoal

This is a by-product of agro and forestry-based residue generated using a small amount of oxygen. The quality or composition of the charcoal powder depends on the original material and can have various numbers of chemical characterisations; however, most of them are interrelated with pure carbon content. The charcoal itself is big and heavy, but the mechanical process breaks it down and produces a powder-like material that settles at the bottom. During transfer or movement, these fine particles escape into the atmosphere and are transported by wind to another location. This material is opaque, and when deposited on PV, it will decimate light transmittance to PV cells. The results below highlight the effect of charcoal powder accumulation on PV performance.

Fig. 12 shows the spectral transmission, SEM and PV performance when coupons (acrylic plastic and glass) were deposited with charcoal. A decrease in light transmission was recorded when charcoal dust was dry deposited on coupons by about 77% on acrylic and 35% on the low iron glass. On the other hand, highier reductions were recorded when charcoal was wet deposited on coupons with acrylic plastic recording about 98% and low iron glass almost 100%. The image characterisation shows that charcoal is a dark compound characterised with opaque minerals that have absorbance, scattering and attenuation effects on light. These minerals appear to have a high density and are capable of slowing flux intensity. Mineral surfaces seem to be coarse, smaller in size with a few medium sizes, which can cause light attenuation. Particles appear in flaky aggregated triangular glassy like structures and are very light in weight. The PV performance result shows that the short circuit current degraded by 76% when the charcoal sample was dry deposited on the acrylic plastic and about 35% on the low iron glass. A substantial increase in degradation was observed when the charcoal sample was wet deposited on the various coupons where about 98% of degradation was recorded on acrylic plastic and 95% on the low iron glass.

3.6. Clay

Clay is comprised of minuscule particles with high cohesion, dilatancy and plasticity and low permeability. When particles are dry, it becomes solid, but when wet, it becomes sticky because of its high-water retention. Tiny silicates are the main minerals found in clay soil. They are light in weight and can be transported by the wind in the atmosphere to PV surfaces, which can cause a reduction of light transmittance to PV cells. The results below highlight the effect of clay formation on PV performance.

Fig. 13 shows the spectral transmission, SEM and PV performance when coupons (acrylic plastic and glass) were deposited with clay. Reduction in light transmittance was recorded when clay was dry deposited on coupons of about 43% on acrylic plastic and 8% on the low iron glass. On the other hand, high reduction was documented when clay was wet deposited on the coupons with the acrylic plastic

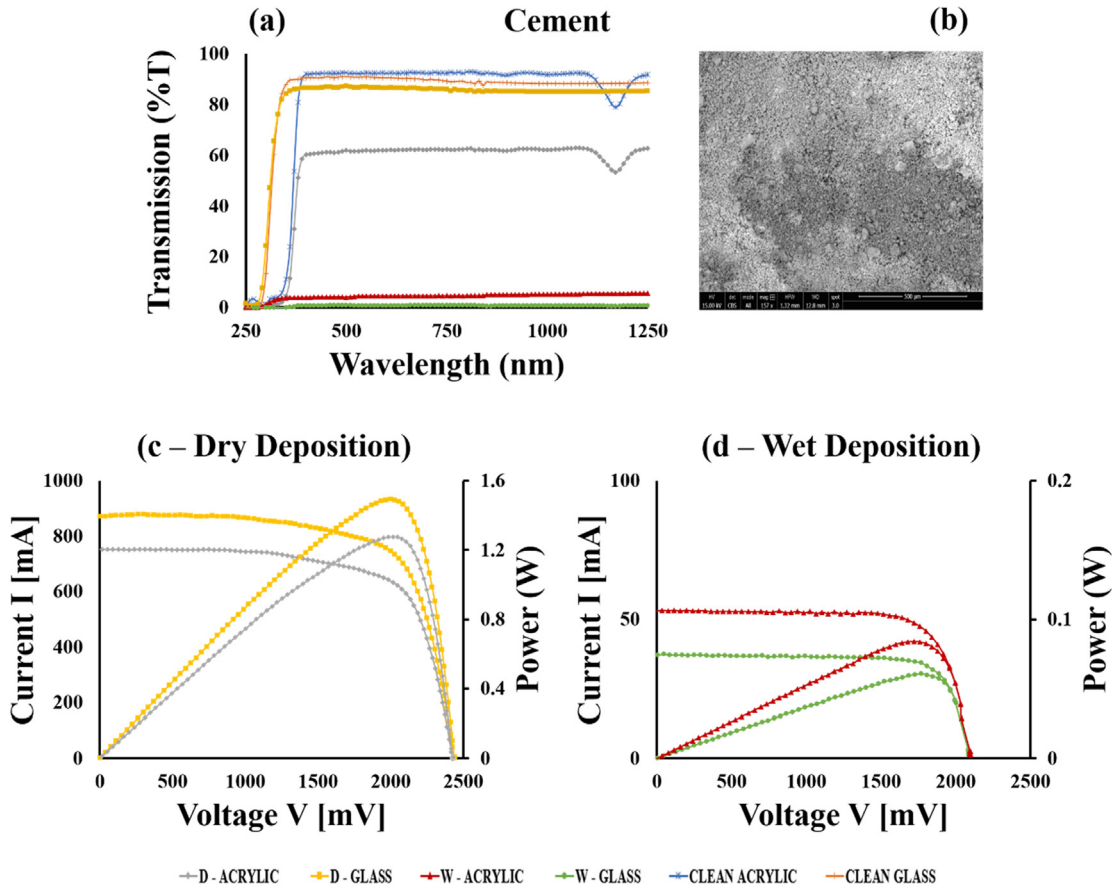

Fig. 11. Cement - (a) Spectral transmittance (b) SEM imaging (c and d) PV performance.

recording about 100% and low iron glass 77%. The image characterisation shows that the clay is comprised of fine minerals that exhibit plasticity and low permeability and appear to be partially translucent and opaque, which has an attenuation effect on light transmittance. Minerals density appears to be high, which can result in reduced flux intensity, causing light absorbance. Particles have smooth and fine surfaces, which can promote scattering, and the shape seems to be a flaky rounded crust structure, which can result in light reflection or attenuation. Particles are very tiny and heavy but can be blown by the wind or gravitational effects, causing rolling, sliding and lift-off. The PV performance result shows that the short circuit current degraded by about 33% when clay samples were dry deposited on acrylic plastic and 14% on the low iron glass. A high increase in degradation was observed when the clay sample was wet deposited on the various coupons where about 96% was recorded on acrylic plastic and 93% on the low iron glass.

3.7. Coarse sand

This is soil mixed with larger pieces of grit that are heavy, and as such cannot be easily transported by wind and hardly stick together even when wet. Coarse sand is described with secondary fraction, larger grain shape, mass structure and density. This material has poor permeability and can hardly settle on a surface. It is difficult to transport, deposit and cement to the surface of a PV module. However, during sandstorms or strong wind, it can be transported and deposited on the module's surface, which can reduce light transmittance to PV cells. The results below highlight the effect of coarse soil formation on PV performance.

Fig. 14 shows the spectral transmission, SEM and PV performance when coupons (acrylic plastic and glass) were deposited with coarse sand. Reduction in light transmittance was recorded when coarse sand was dry deposited on coupons, by about 33% on acrylic plastic and 4% on low iron glass. Reduction was also recorded when coarse sand was wet deposited on coupons with acrylic plastic having about 74%, and low iron glass was about 63%. Image characterisation shows that coarse sand comprising broken rock particles with minerals were translucent and sub translucent, which allows a certain percentage of light to pass through. Mineral density of the minerals appears to be high, which can slow the flux intensity resulting in light absorbance. Particles seem to be heavy, and appear to have a spherical and/or quadrangular structure with a partial coarse surface, which offers favourable optical properties. Although the particles possess some good optical properties, the negative properties surmount. In addition, during both depositions, particles bounce off or roll-off the coupons. The particles are large, meaning this type of dust is porous and light can pass through the spaces. Also, large dust particles can be affected by gravitational forces and light wind effects. The PV performance result shows that the short circuit current degraded by about 17% when the coarse sand sample was dry deposited on the acrylic plastic and by about 10% on the low iron glass coupon. An increase in degradation was observed when the rough sand sample was wet deposited on the various coupons where about 76% degradation was recorded on acrylic plastic and 62% on low iron glass.

3.8. Laterite

This is a reddish, yellowish and/or dark brown soil found in semi-arid or savannah regions with warm air temperatures, dry periods and abundant rainfall such as West Africa, and it comes in different forms because of the iron oxide content. It is used for road construction across the West African region and possesses high level of aluminium and iron, which can harden to form a rock. When mixed with water on a surface,

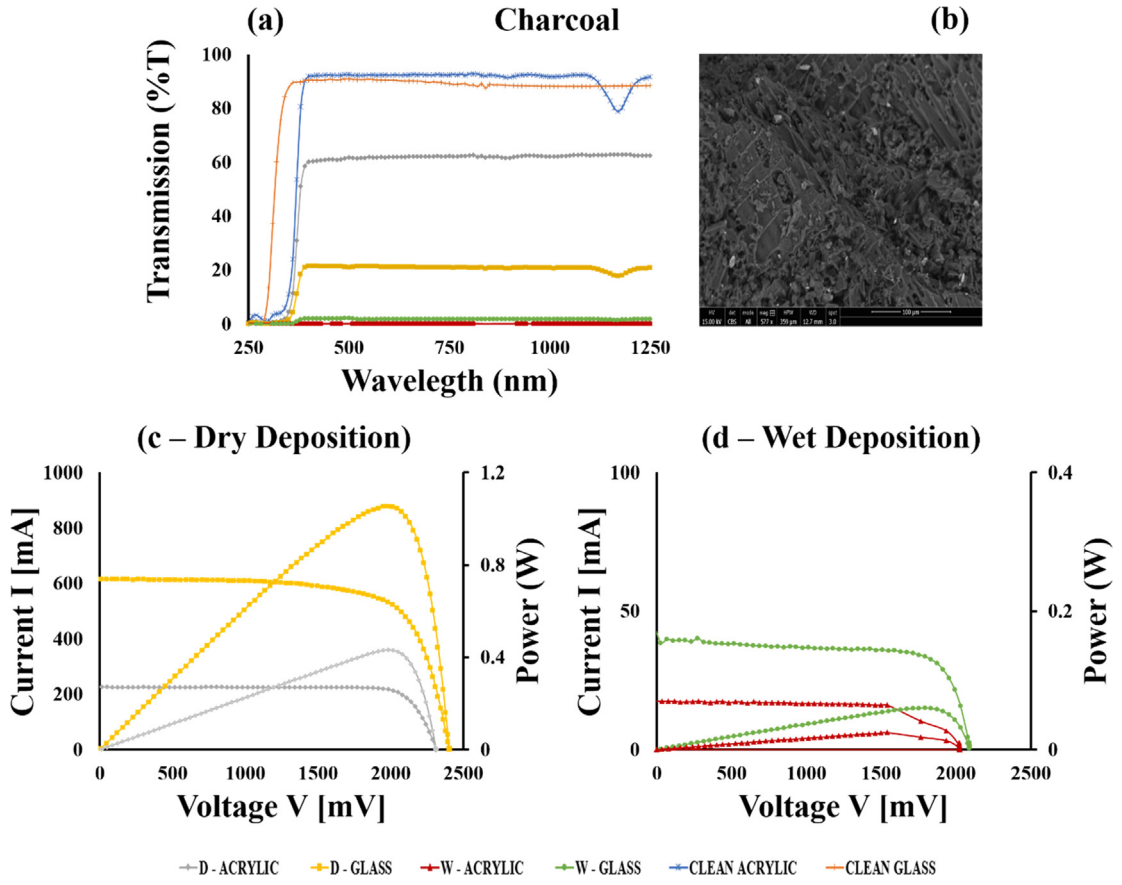

Fig. 12. Charcoal - (a) Spectral transmittance (b) SEM imaging (c and d) PV performance.

it can rapidly dry up, forming cementation. This soil is affected by wind erosion and could be lifted and transported to the module's surface, which can reduce light penetration to PV cells. The results below highlight the effect of lateritic soil formation on PV performance.

Fig. 15 shows the spectral transmission, SEM and PV performance when coupons (acrylic plastic and glass) were deposited with laterite. Light transmittance reduction was recorded when laterite was dry deposited on coupons with acrylic plastic showing about 55% and low iron glass 3% reduction. On the other hand, extreme reduction was documented when laterite was wet deposited on the coupons with both reaching almost 100% reduction. Laterite is a reddish or brownish compound with high levels of aluminium and iron. The image characterisation shows that the mineral content appears to be opaque, translucent and sub translucent, and this characteristic can cause light attenuation. Mineral density was high, which can slow down flux intensity and result in light absorbance. Most of the laterite particles used are tiny, heavy and spherical, which can cause light attenuation, reflection and scattering. Few larger particles bounce off the coupons during deposition. The PV performance result shows that the short circuit current degraded by about 32% when laterite samples were dry deposited on the acrylic plastic coupon and 8% on the low iron glass. An alarming increase in degradation was also observed when laterite sample was wet deposited on the various coupons where about 96% degradation was recorded on acrylic and about 94% on low iron glass.

3.9. Loam

This is a type of soil containing organic components, nutrients and moisture. Loam soil is comprised of sand, silt and clay in different proportions (clay content is very small). It has better water content managing capabilities because it retains a certain amount of water and allows unwanted water to drain away. This soil is less affected by wind erosion. However, it can be lifted and transported by strong wind and storms in the atmosphere and later to the PV module's surface, which can reduce light transmittance to PV cells. The results below highlight the effect of loam soil formation on PV performance.

Fig. 16 shows the spectral transmission, SEM and PV performance when coupons (acrylic plastic and glass) were deposited with loam. Light transmittance reduction was recorded when loam soil was dry deposited on coupons with levels of about 55% for acrylic and 3% for low iron glass. On the other hand, extreme reduction was documented when loam soil was wet deposited on the coupons with both having almost 100% reduction. The image characterisation shows that loam is a compound comprised of various minerals, and some were observed to be opaque and translucent, which can cause light attenuation. Minerals were also found to have a high density, which can reduce flux intensity, causing light absorbance. Particles vary in size; some appear to be very tiny while others are large; this will cause light attenuation because the smaller particles tend to fill up the porous spaces left by the larger particles. These particles are heavy, angular and quadrangular, with coarse surface. The PV performance result shows that the short circuit current degraded by about 37% when loam soil was dry deposited on acrylic plastic and by about 10% on the low iron glass. An alarming increase in degradation was observed when loam soil was wet deposited on the various coupons with about 96% recorded on the acrylic plastic, and 95% on low iron glass coupon.

3.10. Salt

This is a hygroscopic compound that deliquesces to a gaseous state when the relative humidity is low and becomes droplets when relative humidity is high. This compound can be transported from the sea to the module's surface by wind, and during the transport phase, additional dust particles can be incorporated. Sea salt particles adhere to PV

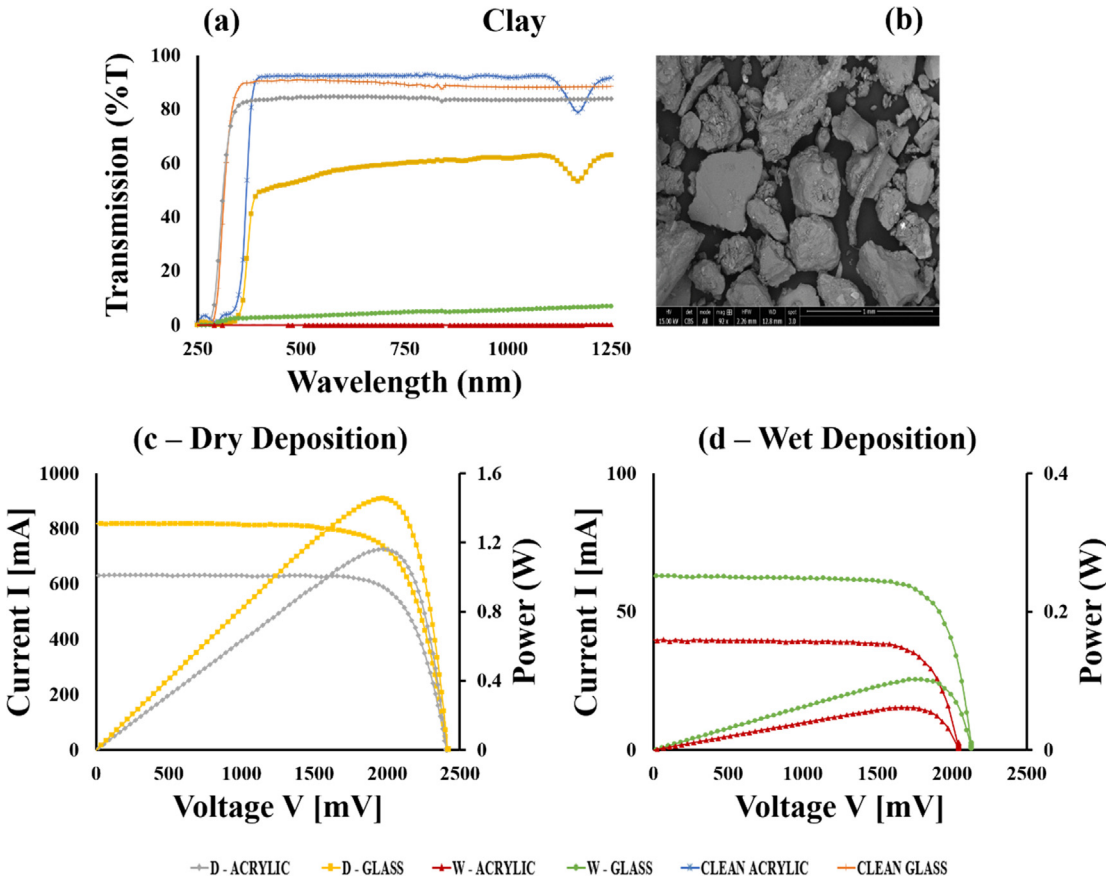

Fig. 13. Clay - (a) Spectral transmittance (b) SEM imaging (c and d) PV performance.

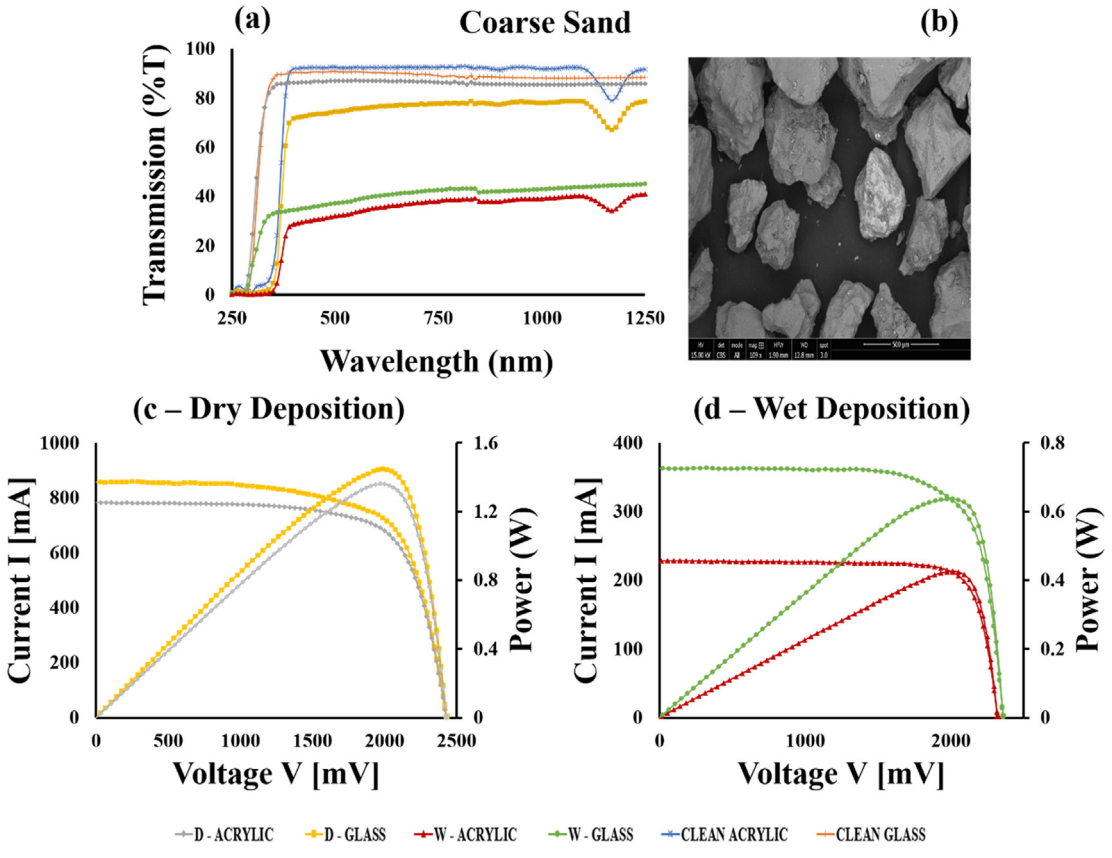

Fig. 14. Coarse sand - (a) Spectral transmittance (b) SEM imaging (c and d) PV performance.

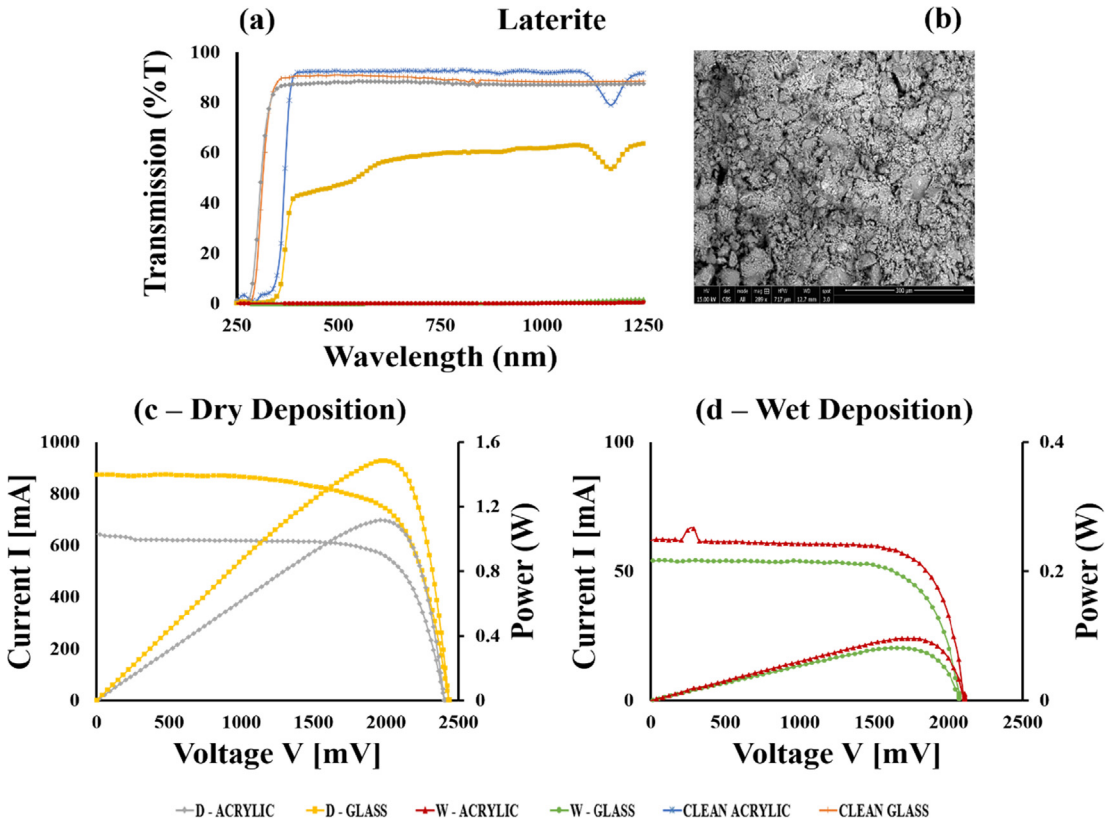

Fig. 15. Laterite - (a) Spectral transmittance (b) SEM imaging (c and d) PV performance.

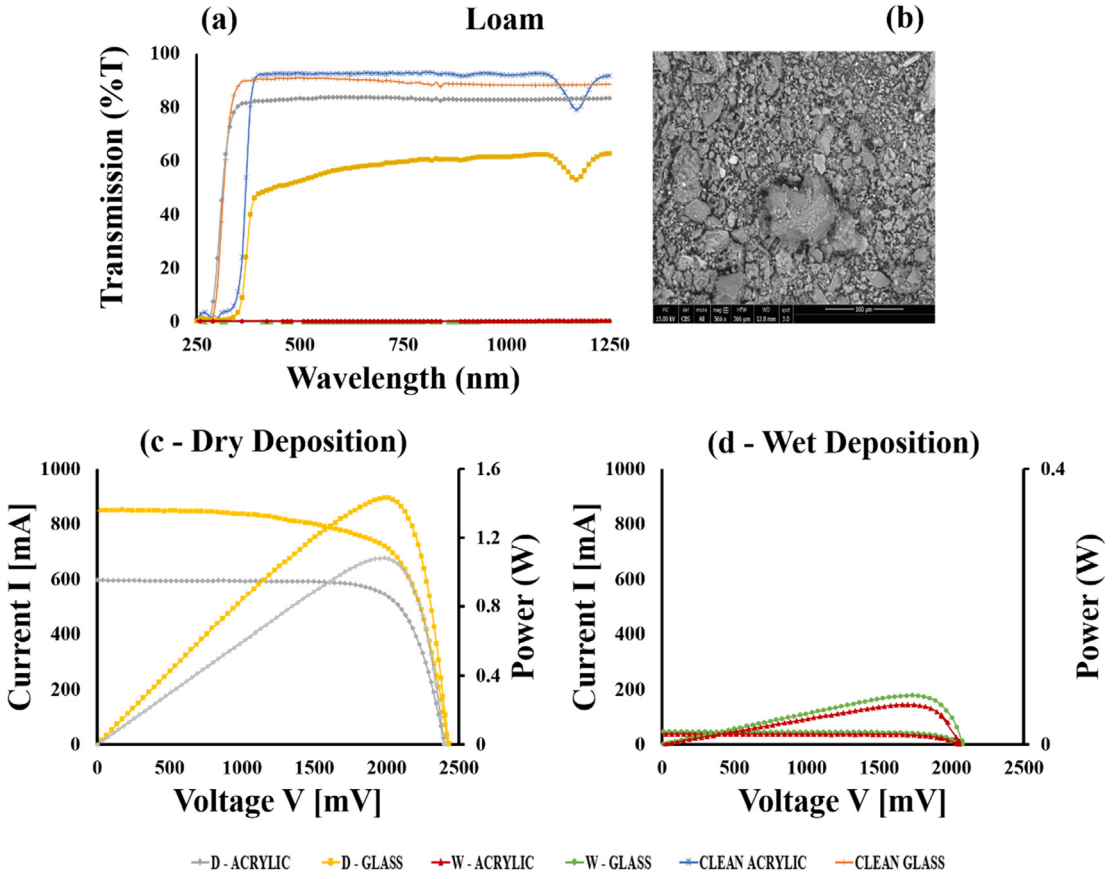

Fig. 16. Loam - (a) Spectral transmittance (b) SEM imaging (c and d) PV performance.

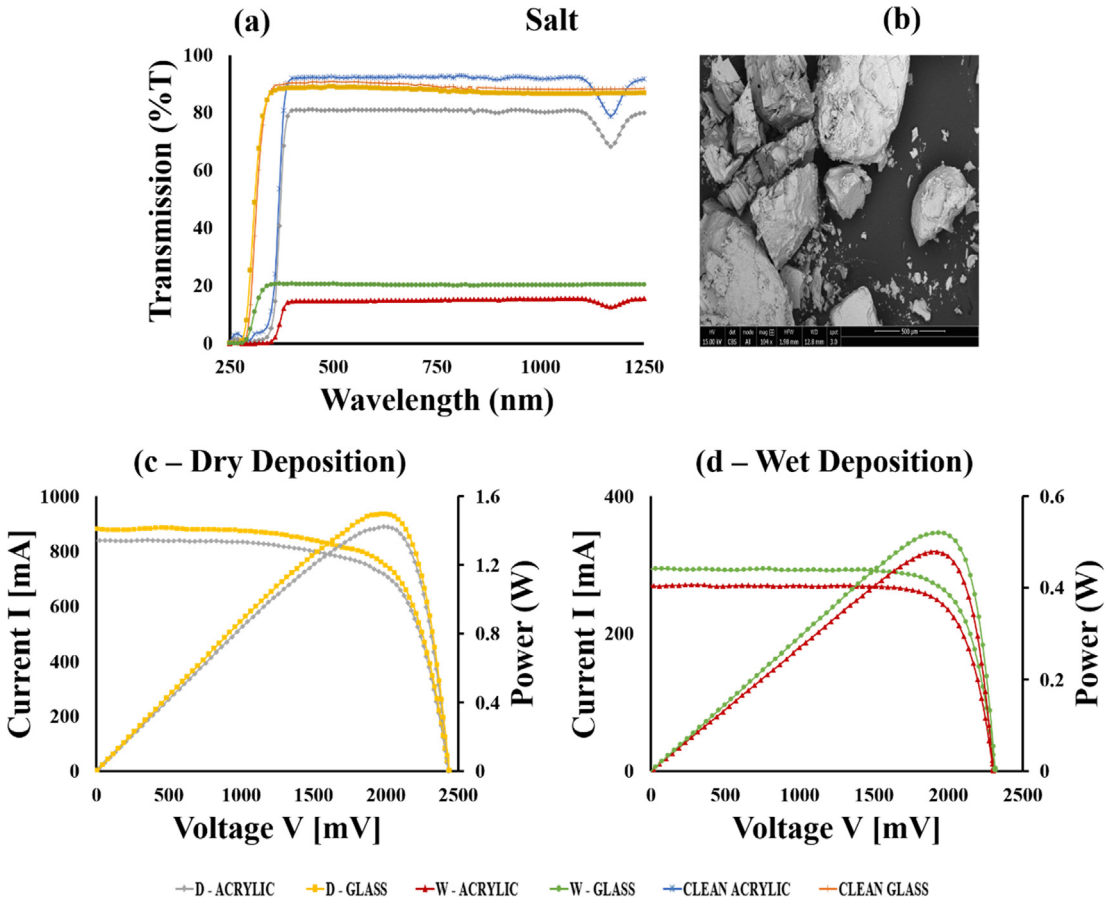

Fig. 17. Salt - (a) Spectral transmittance (b) SEM imaging (c and d) PV performance.

surfaces when they become dry, which can reduce light transmittance to PV cells. The results below highlight the effect of soiling due to sea salt accumulation on PV performance.

Fig. 17 shows the spectral transmission, SEM and PV performance when coupons (acrylic plastic and glass) were deposited with salt. Low light transmittance reduction was recorded when salt was dry deposited on coupons with acrylic plastic showing about 24% and low iron glass about 2% reduction. On the other hand, high reduction was documented when salt was wet deposited on coupons with acrylic plastic recording 87% and low iron glass 77%. The image characterisation shows that salt is a crystalline mineral found to be transparent, with reasonable mineral density; which presents good optical quality since flux intensity will not be affected to a great extent. Particle size ranged from medium to large, which makes it porous, allowing more passage of light. It appears to be a quadrangular layered structure, and its roughness seems to be coarse, which also present good optical properties since better transmittance can be achieved. Despite the good optical qualities salt possesses, negative qualities surmount due to the way it accumulates in layers. The PV performance result shows that the short circuit current degraded by about 12% when salt is dry deposited on acrylic plastic and about 7% on the low iron glass. An increase in degradation was observed when salt was wet deposited on the various coupons where about 72% was recorded on the acrylic plastic and about 69% on the low iron glass coupon.

3.11. Sandy soil

This is fine sand particles used in combination with other materials for plastering or rendering the exterior of a building or structure, found from river beds and riverbanks. It allows water to settle and has less reduced permeability, is easy to compress and lift when completely dry. This type of soil is affected by wind erosion and can be lifted and transported to the PV module's surface, which can reduce light transmittance to PV cells. The results below highlight the effect of sand soil formation on PV performance.

Fig. 18 shows the spectral transmission, SEM and PV performance when coupons (acrylic plastic and glass) were deposited with sand. Light transmittance reduction was recorded when sand was dry deposited on coupons with 51% on acrylic plastic and 11% on the low iron glass. On the other hand, high reduction was recorded when sand was wet deposited onto coupons with both recordings at around 99% reduction.

Image characterisation shows that the sand sample appears to be opaque and partially sub translucent. Minerals were found to have a high density, which can slow flux intensity. Particle sizes range from small to medium, which can cause light attenuation. Particle structure appears to be aggregated and euhedral, so can absorb light. The surface appears to be smooth, causing light scattering. It is also heavy, which means it will readily settle and accumulate on a platform. The PV performance result shows that the short circuit current degraded by about 30% when sandy soil was dry deposited on acrylic plastic and by about 13% on the low iron glass. A substantial increase in degradation was observed when sandy soil was wet deposited on the various coupons, with about 95% degradation recorded on acrylic, and about 94% on the low iron glass.

3.12. Stone dust

This is a quarry industrial by-product, also known as quarry dust; it is grey and can be fine and coarse depending on the holes and screening traps of the crusher used. It is used for road construction, pavement, tiles and bricks due to its highly reduced permeability. Fine stone dust

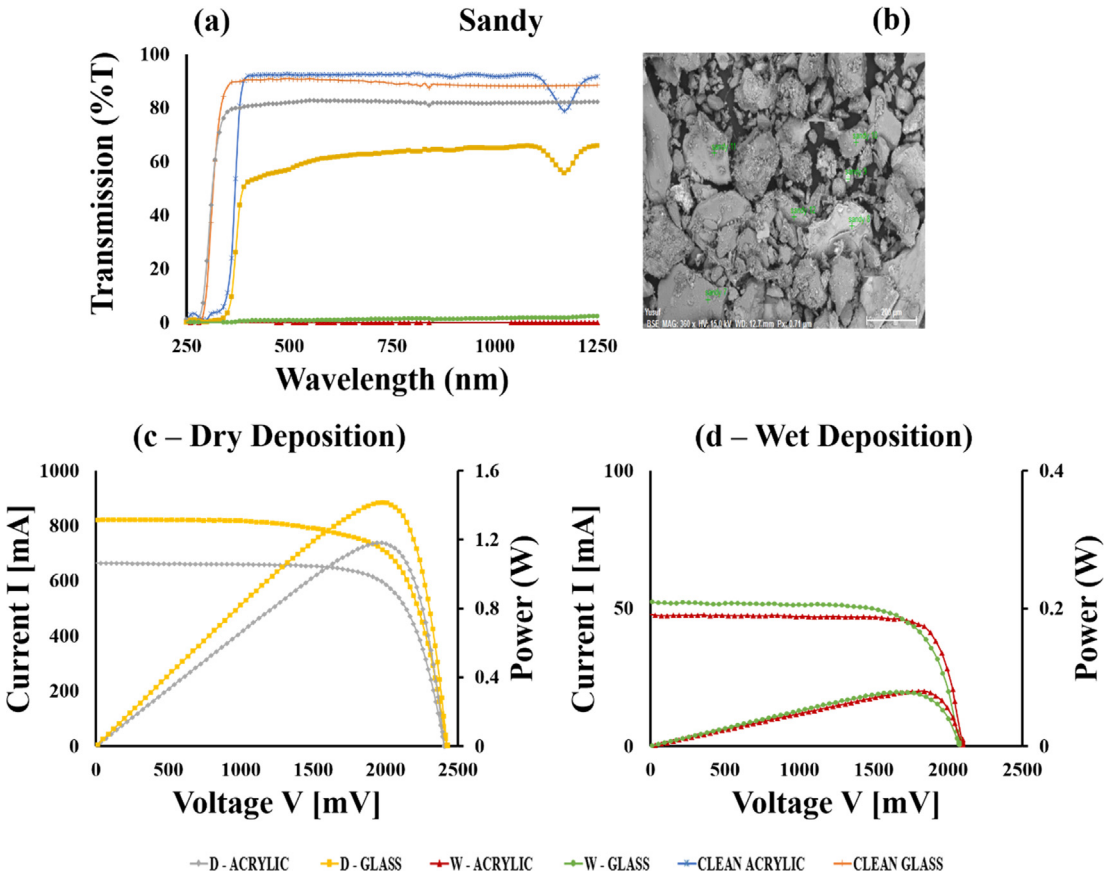

Fig. 18. Sandy - (a) Spectral transmittance (b) SEM imaging (c and d) PV performance.

was selected and used in this research since wind can lift and transport it. Heavier and larger particles are difficult to transport, deposit and cement on the PV module's surface. However, during sandstorms or strong wind, it can be transported and deposited on the module and can reduce light transmittance to PV cells. The results below highlight the effect of stone dust formation on PV performance.

Fig. 19 shows the spectral transmission, SEM and PV performance when coupons (acrylic plastic and glass) were deposited with stone dust. Low light transmittance reduction was recorded when stone dust was dry deposited on coupons with acrylic plastic showing about 16% and low iron glass 5%. On the other hand, high reduction was recorded when stone dust was wet deposited on coupons with acrylic plastic recording 87% and low iron glass as high as 100% reduction. The image characterisation shows that stone dust is comprised of minerals found to be opaque and translucent which have attenuation and reflection effects on light and have a high density which can reduce flux intensity resulting in light absorbance. Particle surfaces appear to be coarse. The structure seems to be an aggregated layer, which can have a scattering effect on light. The stone dust sample used appears to be small and medium sized with low light porosity. It is also heavy, which means it will readily settle and accumulate on a platform but can roll, slide and lift-off due to wind and/or gravitational effects. The PV performance result shows that the short circuit current degraded by about 18% when stone dust was dry deposited on acrylic plastic and by about 9% on the low iron glass. An alarming increase in degradation was observed when stone dust was wet deposited on the various coupons with about 92% degradation recorded on acrylic plastic and about 91% on the low iron glass.

3.13. Wood dust

This is a by-product of wood which is also known as sawdust generated from the carpentry industry when machines are used in cutting, drilling, sawing, milling, roughening and shaping wood. It is a bio-polymeric composite, and some of the fine wood dust become particles are immediately suspended in the atmosphere as they are generated, while others are affected by gravitational forces before a strong wind suspends them in the atmosphere. These particles can be transported to the module's surface and reduce light transmittance to PV cells. The results below highlight the effect of wood dust formation on PV performance.

Fig. 20 shows the spectral transmission, SEM and PV performance when coupons (acrylic plastic and glass) were deposited with wood dust. Light transmittance reduction was recorded when wood dust was dry deposited on coupons with acrylic plastic showing about 56% and low iron glass about 9% reduction. On the other hand, high degradation of light transmittance was recorded when wood dust was dry deposited with both coupons recording about 100% reduction. Image characterisation shows that wood dust (also known as sawdust as mentioned above) is comprised of minerals found to be opaque and translucent, which have an attenuation effect on light, and a high density, which can reduce flux intensity resulting in light absorbance. Particle shape appears to be flaky elongated rectangular structure with a fine surface, which can cause a scattering effect. Particles are light in weight and range from small to medium size, which resulted in an attenuation effect. The PV performance result shows that the short circuit current degraded by about 36% when wood dust was dry deposited on acrylic plastic and about 12% on the low iron glass. Substantial increase in degradation was observed when wood dust was wet deposited on the various coupons with about 92% degradation recorded on acrylic plastic, and about 94% on low iron glass.

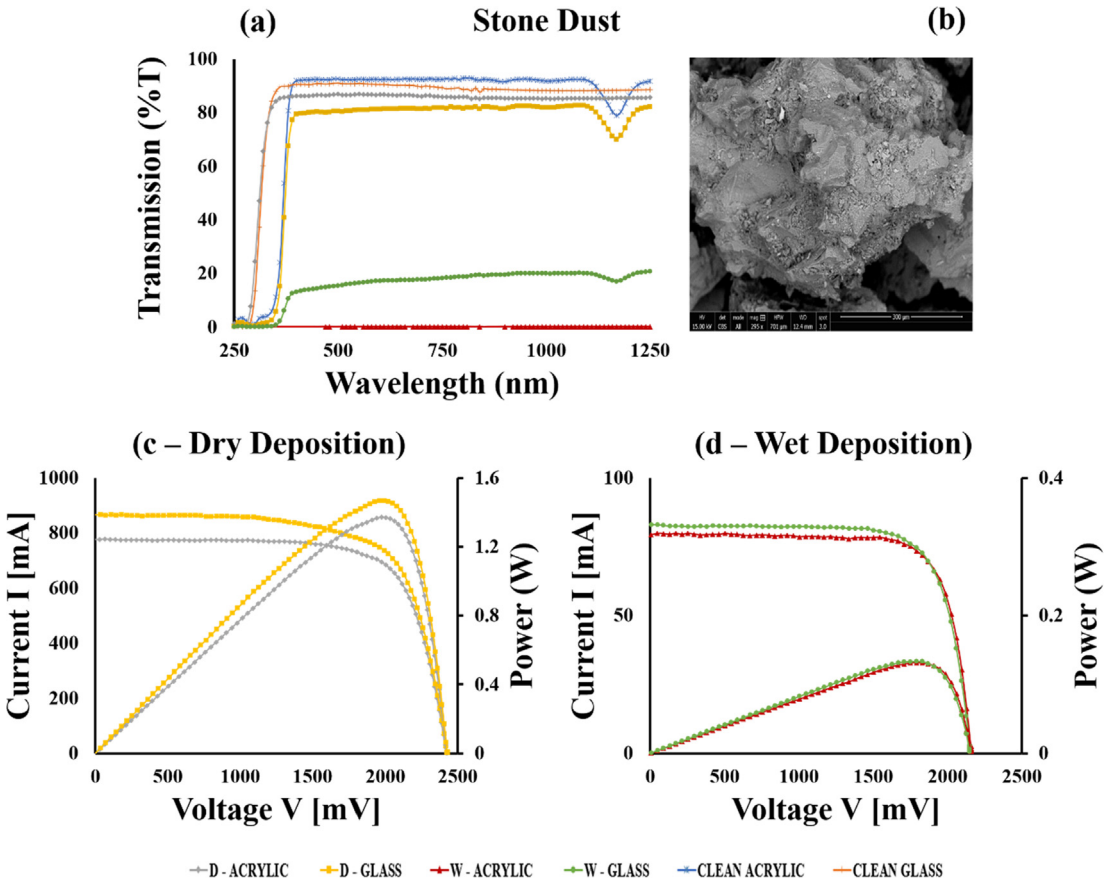

Fig. 19. Stone dust - (a) Spectral transmittance (b) SEM imaging (c and d) PV performance.

3.14. Summary of results

Fig. 21 illustrates the power performance of the module when different dust types were deposited onto the PV surfaces. In addition, Table 3 illustrates the short circuit current degradation of each sample, power degradation, transmission losses, and results from image characterisation.

4. Discussion

Alarming results were highlighted in the previous section, some of them showing almost 100% degradation of performance. Several parameters were considered to characterise and analyse each variety of dust particle in addition to how and what promotes its degradation effect on PV cell performance. This section provides an in-depth discussion of the analysed results from the various experiments.

This research investigated two materials (acrylic plastic and low iron glass) used in the PV industry for encapsulating solar cells and which allow adequate light transmittance for the functioning of the technology. These materials were selected since they possess excellent transmittance quality. Acrylic has a transmittance of about 92%, and low iron glass has a transmittance of 91%. These materials have many other advantages that have made them an effective option in the industry. Results from the literature and laboratory experiments show that the acrylic plastic possesses a higher transmittance capability than the low iron glass. However, results also show that the acrylic plastic attracts and accumulates more dust during depositions. This is due to electrostatic discharge (ESD) of the material, which attracts the particles. This claim is supported by Zaihidee et al. (2016), and Jiang et al. (2011), who stated that plastic and epoxy materials could accumulate more dust than glass. This result is comparable with a report provided by Nahar and Gupta (1990), where acrylic plastic was found to accumulate a greater amount of dust when compared to a glass surface. A report provided by Kalogirou et al. (2013) also confirmed that glass was found to accumulate less dust compared to Tedlar.

The image analysis comprising of morphological and mineral characterisation of particles describes the size, weight, shape, surface roughness and mineral composition (including their diaphaneity and density). These properties vary with minerals, and most samples are comprised of more than two minerals, excluding salt. However, the negative properties surmount the positive ones and have more influence on light transmittance due to accumulation.

Our result revealed that larger particles create wider gaps between them and could allow light to pass through the gaps, but small and uniformly spread particles would not have enough spaces that light can penetrate. Adıgüzel et al. (2019) investigated the effect of different sizes of coal dust particles on PV performance, their results showed that most significant power losses were observed when the smaller particles of coal dust were deposited in comparison to larger particles. They also proved that increasing the weight of accumulated dust particles further reduces the yield of the technology. A micro or nano-sized particle can prevent a tiny fraction of solar radiation from reaching the solar cell, which is essential for its operation, thereby degrading the overall performance of the technology. The results presented in Table 3 are compatible with other experimental studies highlighted in Table 4, which shows that certain dust particles cause reduction of transmittance and decrease in PV output. It should be noted that the actual quantity used by other researchers presented in Table 4 were minimal whereas a large quantity was used in this experiment which was an informed decision based on an observation made in an ongoing study and other outdoor soiling experimental publications.

Al-Ammri et al. (2013) investigated the effect of bird droppings

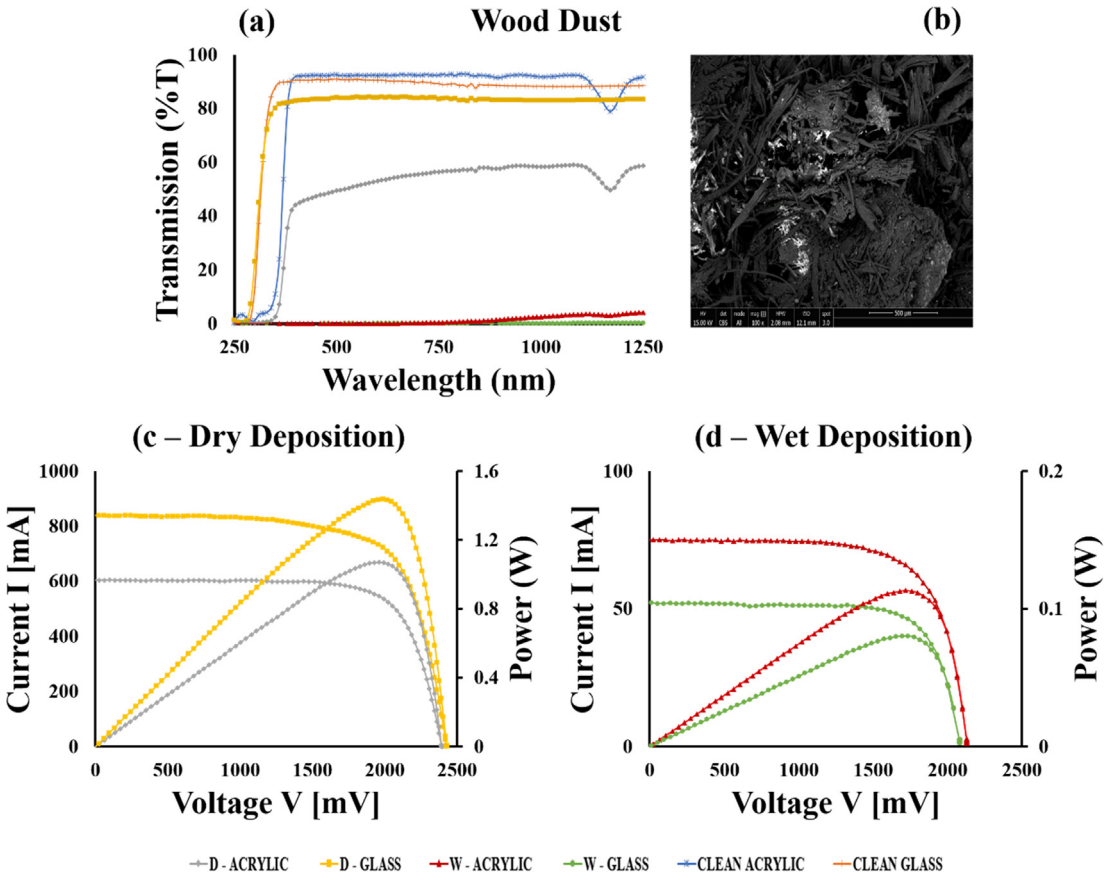

Fig. 20. Wood dust - (a) Spectral transmittance (b) SEM imaging (c and d) PV performance.

deposition on PV performance and reported that bird droppings deposition had a greater effect than dust. On the contrary, our study found that a dust sample (charcoal) deposition had a greater effect on PV performance when compared to bird droppings. In addition, El-Shobokshy and Hussein (1993) reported that carbon particles absorb more solar radiation compared to limestone and cement. Similarly, this research also shows that samples with carbon particles (charcoal) absorbed more light compared to cement.

It is observed that particles were rolling, sliding and lifted off the coupons when exposed to artificially generated wind velocity and gravitational effect (when coupons were tilted). The results show that wind and gravitation effect have more effect on the dry deposited dust when compared to the wet deposited samples.

The effect of dust particle deposition (dry and wet) processes have been compared, and the results are highlighted in the diagrams above. Our results illustrate how dry and wet deposition can affect light transmittance. It was observed that during the dry deposition on the coupons, (acrylic plastic and low iron glass) a small quantity of tiny samples particles adhered to the coupons. Theoretically, it has been established that Van de Waal forces are always present between the particles and the surface, which can act together when the interacting dipoles are within short range (Ilse et al., 2018). This factor can influence the adhesion of dry dust on both coupons. The electrostatic force that is always present on the acrylic plastic is another factor that can attract the dust during dry deposition, leading to more dust accumulation resulting in greater PV performance degradation than that of

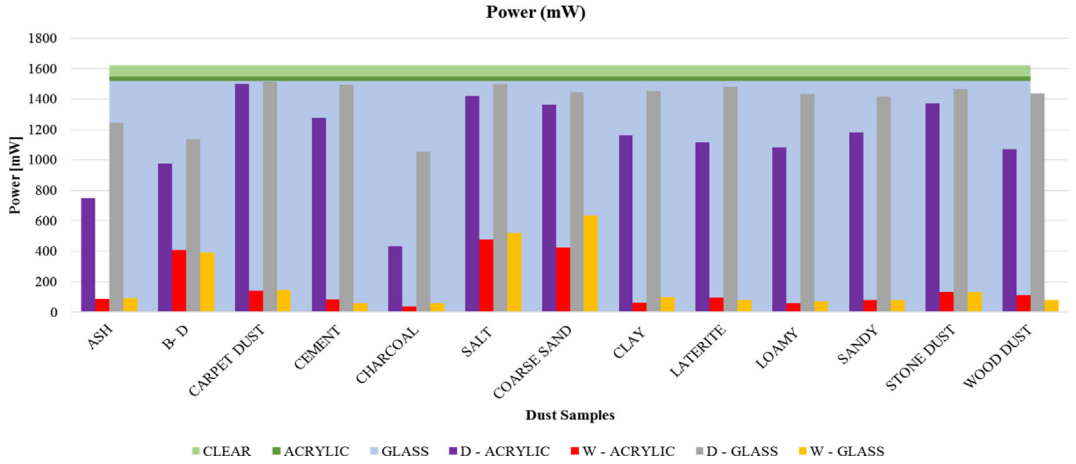

Fig. 21. Summary of results (power output).

Table 3
Summary of results.

	I_{sc} degradation				Power degradation				Transmission degradation				Image characterisation						
	Acrylic		Glass		Acrylic		Glass		Acrylic		Glass								
	Dry%	Wet%	Dry%	Wet%	Dry%	Wet%	Dry%	Wet%	Dry%	Wet%	Dry%	Wet%	Size(mm)	Weight(g/m^2)	Shape structure	Surface roughness	Composition	Diaphaneity	Density
ASH	56	94	22	94	54	95	23	94	55	99	4	87	0.5–80	1289.94	Angular	Coarse	Fairchildite	Transparent	2.45
																	Manganese	Opaque	7.01
B-D	46	87	35	74	40	75	30	76	90	87	54	75	0.1–400	958.58	Aggregate	Fine	Amphibole (Richterite)	Translucent	3.09
																	Silica	Opaque	2.13
																	Xenotime	Transparent	
CARPET	9	91	7	92	8	91	7	91	8	100	1	100	< 1- > 1000	609.47	Bent angular/triangular channels	Coarse	Olivine (monticellite)	Translucent	3.13
																	Calcite	Opaque	2.71
CEMENT	21	94	8	96	21	95	8	96	34	95	4	99	< 1–150	1964.50	Angular flattened	Coarse	Hatrurite	Opaque	3.02
																	Brownmillerite	Semi Transparent	3.76
																	Calcite	Opaque	2.71
CHARCOAL	76	98	35	95	73	98	35	96	77	98	35	100	< 1–100	923.08	Flaky aggregated triangular glassy like	Coarse	Ankerite	Sub Translucent	3.05
																	Calcite	Opaque	2.71
																	Charcoal	Opaque	
CLAY	33	96	14	93	28	96	10	94	43	100	8	77	< 2- < 60	2621.30	Flaky rounded crust	Fine	Beryl	Translucent	2.76
																	Stilpnomelane	Opaque	2.86
																	Anxite	Translucent	3.28
COARSE	17	76	10	62	16	74	11	61	33	74	4	63	50–2000	3218.93	Rounded and quadrangular structure	Coarse	Allanite	Translucent	3.93
																	Chlorite (Chamosite)	Sub Translucent	3.2
																	Prehnite	Translucent	2.87
LATERITE	32	93	8	94	31	94	9	95	55	100	3	100	> 50–150	2426.04	Aggregated angular and rounded layered	Coarse	Schorl	Opaque	3.15
																	Chlorite (Chamosite)	Sub Translucent	3.2
																	Bauxite	Opaque	3.5
LOAMY	37	96	10	95	33	96	12	96	55	100	9	100	< 2–2000	3011.83	Angular and quadrangular	Coarse	Feldspar (Labradorite)	Translucent	2.69
																	Stilpnomelane	Opaque	2.86
																	Anxite	Translucent	3.28
SALT	12	72	7	69	12	70	8	68	24	87	2	77	50–500	2846.15	Quadrangular layered	Coarse	Halite	Transparent	2.17
SAND	30	95	13	94	27	95	13	95	51	99	11	100	15–500	2384.62	Aggregated euhedral	Fine	Mica (Biotite)	Opaque	3.9
																	Beryl	Translucent	2.76
																	Stilpnomelane	Opaque	2.86
STONE	18	92	9	91	16	92	10	92	16	87	5	100	75–250	2751.48	Aggregated layered	Coarse	Mica (Muscovite)	Translucent	2.82
																	Staurolite	Opaque	3.71
																	Leucite	Translucent	2.47
WOOD	36	92	12	94	34	93	12	95	56	100	9	100	10–100	609.47	Elongated flaky rectangular like	Fine	Calcite	Opaque	2.71
																	Beryl	Translucent	2.76

Table 4
Results from similar research.

Authors	Particles samples	Quantity	Output percentage reduction	Transmittance reduction
Alnasser et al. (2020)	Sand	100 g/m^2	12%	40% @ 35 g/m^2
▪ Power reduction (%)	Normal cement	100 g/m^2	14%	45% @ 35 g/m^2
▪ Transmittance reduction (%)	White cement	100 g/m^2	15%	55% @ 35 g/m^2
	Normal gypsum	100 g/m^2	9%	50% @ 35 g/m^2
	Technical Gypsum	100 g/m^2	10%	52% @ 35 g/m^2
Kaldellis et al. (2011)	Red soil	0.35 g/m^2	0.75%	
▪ Efficiency reduction (%)	Limestone	1.51 g/m^2	0.95%	
	Fly ash	3.71 g/m^2	1.5%	
Kazem et al. (2013)	Red soil	10 g/m^2	7%	
▪ Power reduction (%)	Ash	10 g/m^2	25%	
	Sand	10 g/m^2	4%	
	Calcium Carbonate	10 g/m^2	5%	
	Silica gel	10 g/m^2	4.5%	
Appels et al. (2013)	White sand	60 g/m^2	14.74% and 13.76%	15.03
▪ Power reduction (%)	Clay	60 g/m^2	48.77% and 47.21%	48.42
▪ Transmittance reduction (%)	Cement	60 g/m^2	64.16% and 65.68%	66.66
Abderrezek and Fathi (2017)Transmittance reduction (%)	Ash	1.02 g/m^2		73.71%
	Cement	1.01 g/m^2		74.62%
	Gypsum	1.01 g/m^2		65.52%
	Salt	1.2 g/m^2		62.79%
	Soil	1.02 g/m^2		20.02%
	Sand	1 g/m^2		19.11%
El-Shobokshy and Hussein (1993)	Carbon	28 g/m^2	90%	
▪ Power reduction (%) @ 195 W/m^2	Cement	73 g/m^2	80%	
▪ I_{sc} reduction (%) @ 195 W/m^2	Limestone (50 μm)	125 g/m^2	80%	
	Limestone (60 μm)	168 g/m^2	78%	
	Limestone (80 μm)	250 g/m^2	94%	
Wang et al. (2020a,b)	Sand	2.199 g/m^2	5.296%	
▪ Efficiency reduction (%)		6.29 g/m^2	12.027%	
		17.37 g/m^2	34.332%	
		21.067 g/m^2	38.981%	
		30.18 g/m^2	43.216%	
Sisodia and Mathur (2019)	Bird dropping		23.8% @ 0^0	31% @ 0^0
▪ Reduction in power (%) with tilt angle β			23.8% @ 10^0	28% @ 10^0
▪ Reduction in transmittance (%) with tilt angle β			21.0% @ 20^0	27% @ 20^0
			11.5% @ 25^0	15% @ 25^0
			10.8% @ 30^0	14% @ 30^0
			10.5% @ 40^0	13% @ 40^0
			10.8% @ 50^0	14% @ 50^0
			10.8% @ 60^0	15% @ 60^0
			15.8% @ 70^0	18% @ 70^0
			16.0% @ 80^0	21% @ 80^0
			16.5% @ 90^0	24% @ 90^0
Adıgüzel et al. (2019)	Coal dust 38 μm	15 g	62.05%	
▪ Power reduction (%)	Coal dust 38–53 μm	15 g	55.78%	
	Coal dust 53–75 μm	15 g	50.83%	
	Coal dust 75–106 μm	15 g	44.12%	
	Coal dust 106–250 μm	15 g	36.97%	
	Coal dust 250–500 μm	15 g	28.90%	

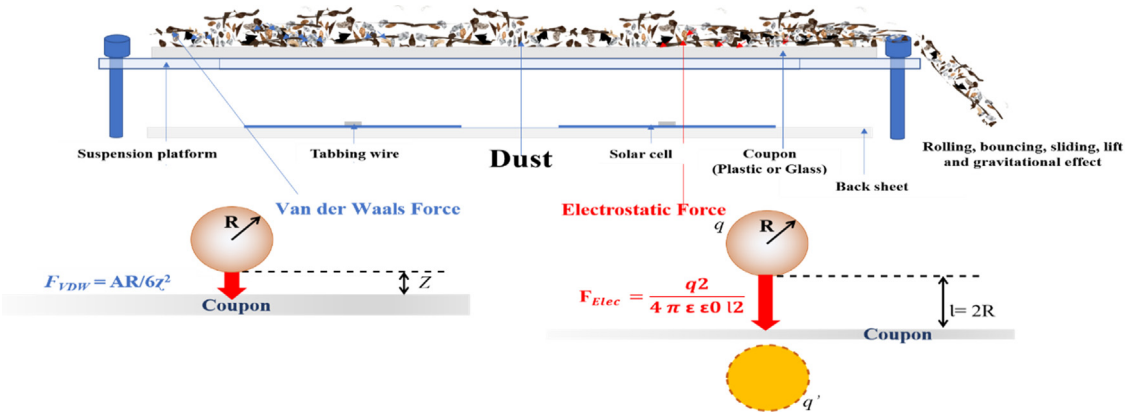

Fig. 22. VDW and Electrostatic force promoting dust particles accumulation.

the low iron glass. Fig. 22 illustrates how the Van der Waals and Electrostatic force acted between particles and the surface.

Where R represents the radius of dust particles, ρ is material density, q is the charge of a particle, A is the Hamaker constant, ζ is the distance between the particle and coupon, ι is separation distance, ε is the dielectric constant that exists between the surface and particles, εo is the free space permittivity (Isaifan et al., 2019).

The adhesion caused during the dry deposition, which was due to the gravitational, electrostatic and Van der Waal forces was compatible with results presented by Isaifan et al. (2019). On the contrary, the main active forces causing adhesion during the wet deposition were gravitational, capillary and Van der Waal forces. This result is compatible with those presented by Isaifan et al. (2019), where the researchers stated that capillary force accounts for about 98% of the forces acting during the humid condition (wet deposition), while 2% was due to Van der Waal forces.

The electrostatic force could promote inter-particle adhesion during a deposition where charged particles collide with one another or the surface, inducing a coulomb force and attracting each other due to opposite charges. When a coulomb force is triggered, it may attract or repulse, depending on the polarity of the dust particle. It was observed that the adhesion is higher between particles compared to the PV surface and particles. Hassan et al. (2016) confirmed that the existence of electrostatic charges could cause tiny particles to adhere to the large ones. In addition, Kazmerski et al. (2016) reported that the adhesion force between particles and PV surfaces is lower when compared to the inter-particle adhesion force.

On the other hand, it was observed that during the wet deposition of samples, additional forces increase the adhesion. The main forces that promoted adhesion on acrylic plastic during this deposition were the capillary force and electrostatic force. The electrostatic forces attracted particles to remain on the coupon's surface while the capillary forces created bridges that caused mechanical interlocking of the particles and surface. Since particles were allowed to settle for over 24 h, then cementation, caking and capillary ageing occur. On the other hand, the adhesion force that acted on the low iron glass was capillary. As mentioned above, it created capillary bridges between the particles and coupons, causing entanglement/mechanical interlocking. Furthermore, since particles were allowed to settle over a long period, cementation, caking and capillary ageing occurs. More PV degradation was observed during wet deposition on the acrylic plastic, except for a few samples (such as carpet dust, cement, laterite and wood) that caused slightly greater PV performance degradation on low iron glass than the acrylic plastic. Fig. 23 illustrates how the capillary force acted on dust particles when water was introduced.

Where γ is the surface tension and θ is the contact angle between the moisture and coupon (Isaifan et al., 2019).

The overall results show that the presence of water on the PV surface promotes bonding and adhesion potency both between particles and also between particles and module surface materials due to triggering of capillary forces, preventing the sliding, bouncing off, lift and rolling off of particles which leads to retention of more particles on the module surface. Light rain, high relative humidity and dew are ways of depositing water droplets with dust particles on the PV surface, and the dew could occur in the early hours of the morning. After sunshine, the particles will dry up to and become firmly adhered to each other and the module surface (cementation), making it very difficult to clean. Depositing water before and after, during the wet deposition creates a stronger adhesion between particles and the coupons that leads to a massive increase in PV yield degradation. Ilse et al. (2018) confirmed this by stating that dew enhances adhesion of accumulated dust on the PV module's surfaces and some particles might improve the strength of the adhesion depending on the chemical composition. In addition, Said and Walwil (2014) stated that the existence of water between the dust particles creates capillary bridges both between the particles and between dust particles and the surface.

Exposing accumulated particles to the wind shows a significant removal effect on dry accumulated dust, but less effect was observed when wet deposited particles were subjected to wind. As earlier stated, Gholami et al. (2017) reported that when accumulated dust particles are subjected to an inward wind, the density of dust particles was reduced. We also observed that large particles (such as coarse sand) were removed when coupons were tilted and exposed to the wind, and the microscopic particles remained on the surface. Jiang et al. (2018) reported that the wind effect is more significant to larger dust structures compared to smaller ones. Tanesab et al. (2019) also reported that it is challenging to remove the tiny layer of dust particles on a PV module that is horizontally positioned.

PV performance relies on solar irradiance, and this research observed that the short circuit current is influenced by dust accumulation, reducing the PV yield. Overall, the PV performance results show that the short circuit current is significantly affected compared to open-circuit voltage since the short circuit current depends on light illumination while voltage is affected by temperature. The highest reduction of short circuit current was observed when the charcoal sample was wet deposited on acrylic plastic while the lowest reduction was when salt was dry deposited on the low iron glass coupon. The observed reductions in short circuit current resulted in a similar reductions in the overall power output of the mini-module. The result obtained from the transmittance test was used in validating the losses that were observed. Dust accumulation on the PV surface reduces the conversion efficiency of the system since the accumulated particles can scatter, absorb and

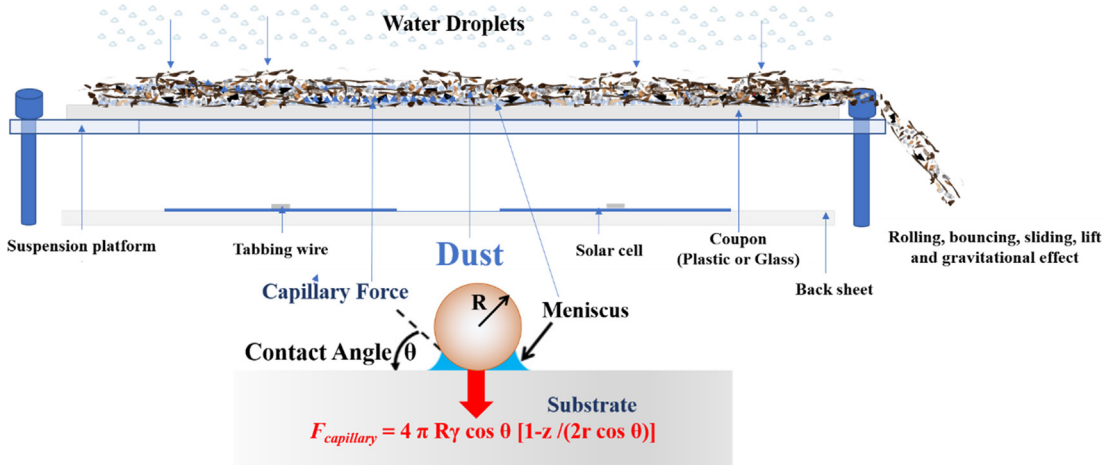

Fig. 23. Capillary force promoting dust particle accumulation.

attenuate incident light from reaching the solar cell. All the samples used in this research reduce or prevent light from reaching the solar cell and decreasing the conversion efficiency of the system. However, this report shows that physical and chemical characteristics of a particle play a significant role in determining the level of degradation it can cause. The results presented highlight that the degradation of PV yield performance caused by dust accumulation depends not only on the amount of dust but also on the physical and chemical properties of the dust particles. This has also been confirmed by Kazem and Chaichan (2019) and Sarver et al. (2013). Hachicha et al. (2019) stated that physical and chemical composition is an essential factor that determines how particles interact with each other and with PV module's surfaces. Previously, researchers have also stated that it would be beneficial to determine the most effective technique to mitigate dust accumulation. Gupta et al. (2019) stated that there is no recommended rate of cleaning since dust accumulation is depending on several variables. Several mitigation techniques such as manual cleaning, the natural method by wind and rain, mechanical and robotics and self-cleaning using the electrodynamic screens, superhydrophobic and super hydrophilic coating were provided by Chanchangi et al. (2020). These approaches are location-dependent, and each one has its limitation. Therefore, there is a need to conduct another research using specific environment condition to determine an efficient practical approach for a specific location. This study provides a thorough analysis of the effect of dust properties on PV performance and could be used for site selection and in planning solar PV farm design. Results from this study could also be used in choosing suitable mitigation techniques according to location and consideration of other factors. The asperity of degradation observed in this study cannot be overlooked, and therefore proper mitigation techniques must be provided to prevent soiling of PV surfaces.

5. Conclusion

Dust property is among the factors influencing dust formation on PV, causing degradation of its performance. This research presented a detailed indoor experimental study of the effect of 13 dust samples on PV performance, considering two different PV surfaces and using two deposition conditions. According to the results obtained, the following conclusions have been drawn:

- Charcoal powder has the greatest effect on light transmittance, affecting short circuit current, and causing the most significant degradation in PV yield performance (98% power reduction) while salt was found to be the lowest (7% power output reduction).
- Few dust particles (such as salt, coarse, carpet dust and cement) appear to possess good optical characteristics, but the negative attributes surmount due to accumulation in layers.
- The research identified acrylic plastic as the material that accumulates a higher quantity of dust compared to low iron glass.
- Wet deposition of dust particles (representing dew or light rain) promotes retention of more particles on a surface when compared to dry deposition since the capillary force can create bridges between particles and the surface.

The asperity of all the degradations observed cannot be overlooked, thereby requiring an appropriate mitigation technique to protect or restore the PV performance from soiling and to amplify penetration of the technology so that sustainable development goal 7 (*"Ensure access to affordable, reliable, sustainable and modern energy for all"*) target can be achieved.

Declaration of Competing Interest

The authors declare the following financial interests/personal relationships which may be considered as potential competing interests: This research is financially supported by the PTDF (Petroleum Technology Development Fund) Nigeria, and the authors would like to acknowledge the funding gratefully. This work has been conducted as part of the PhD research which is funded by PTDF. This work has been conducted as part of the research project 'Joint UK-India Clean Energy Centre (JUICE)', which is funded by the RCUK's Energy Programme (contract no: EP/P003605/1). This work was also supported by the EPSRC IAA Grant (Contract No-EP/R511699/1) received by Dr Aritra Ghosh. The research funders were not directly involved in the writing of this article and have no influence or potential competing interest whatsoever regarding this publication. We declare that this work has not been published elsewhere and that it has not been submitted simultaneously for publication elsewhere.

Acknowledgement

The Petroleum Technology Development Fund financially supports this research, through a PhD research grant to Yusuf N. Chanchangi. This work has been conducted as part of the research project 'Joint UK-India Clean Energy Centre (JUICE)', which is funded by the RCUK's Energy Programme (contract no: EP/P003605/1). This work was also supported by the EPSRC IAA Grant (Contract No-EP/R511699/1) received by Dr Aritra Ghosh. In support of open access research, all underlying article materials and data can be accessed upon request via email to the corresponding authors. Authors would like to acknowledge the funding gratefully. The research funders were not directly involved in the writing of this article.

References

Abderrezek, M., Fathi, M., 2017. Experimental study of the dust effect on photovoltaic panels' energy yield. Sol. Energy 142 (2017), 308–320. https://doi.org/10.1016/j.solener.2016.12.040.

Adıgüzel, E., Özer, E., Akgündoğdu, A., Yılmaz, A.E., 2019. Prediction of dust particle size effect on the efficiency of photovoltaic modules with ANFIS: An experimental study in the Aegean region, Turkey. Sol. Energy 177 (2019), 690–702. https://doi.org/10.1016/j.solener.2018.12.012.

Aïssa, B., Isaifan, R.J., Madhavan, V.E., Abdallah, A.A., 2016. Structural and physical properties of the dust particles in Qatar and their influence on the PV panel performance. Sci. Rep.

Alnasser, M.A.T., Mahdy, A.M.J., Abass, K.I., Chaichan, M.T., Kazem, H.A., 2020. Impact of dust ingredient on photovoltaic performance: An experimental study. Sol. Energy 195 (2020), 651–659. https://doi.org/10.1016/j.solener.2019.12.008.

Al-Ammri, A., Ghazi, A., Mustafa, F., 2013. Dust effects on the performance of PV street light in Baghdad city. In: Paper presented at the 2013 International Renewable and Sustainable Energy Conference (IRSEC), Ouarzazate, Morocco. https://ieeexplore.ieee.org/stamp/stamp.jsp?tp=&arnumber=6529687.

Al-Hasan, A.Y., 1998. A new correlation for direct beam solar radiation received by a photovoltaic panel with sand dust accumulated on its surface. Sol. Energy 63 (5), 323–333.

Al-Shabaan, G.S., W.A., Abu-Al-Aish, A., 2016. Effects of dust grain size and density on the monocrystalline PV output power. Int. J. Appl. Sci. Technol. 6(1), 81–86.

Appels, R., Lefevre, B., Herteleer, B., Goverde, H., Beerten, A., Paesen, R., Medts, K., Driesen, J., Poortmans, J., 2013. Effect of soiling on photovoltaic modules. Sol. Energy 96 (2013), 283–291. https://doi.org/10.1016/j.solener.2013.07.017.

Argungu, G.M., More, A.U., Dabai, K.A., Abdulazeez, S., Ahmad, S.K., 2019. Algorithm for the performance evaluation of three selected wind energy conversion systems (WECS) for electricity generation in Minna, Nigeria. Sci. J. Energy Eng. 7 (2), 29–31. https://doi.org/10.11648/j.sjee.20190702.12.

Beattie, N.S., Moir, R.S., Chacko, C., Buffoni, G., Roberts, S.H., Pearsall, N.M., 2012. Understanding the effects of sand and dust accumulation on photovoltaic modules. Renewable Energy 48 (2012), 448–452. https://doi.org/10.1016/j.renene.2012.06.007.

Becher, R., Øvrevik, J., Schwarze, P.E., Nilsen, S., Hongslo, J.K., Bakke, J.V., 2018. Do carpets impair indoor air quality and cause adverse health outcomes: a review. Int. J. Environ. Res. Public Health 15 (184), 1–14.

Costa, S.C.S., Sonia, A., Diniza, A.C., Kazmerskia, L.L., 2018. Solar energy dust and soiling R&D progress: Literature review update for 2016. Renew. Sustain. Energy Rev. 82 (2018), 2504–2536. https://doi.org/10.1016/j.rser.2017.09.015.

Chanchangi, Y.N., Ghosh, A., Sundaram, S., Mallick, T.K., 2020. Dust and PV performance in Nigeria: A review. Renew. Sustain. Energy Rev. 121 (2020), 1. https://doi.org/10.1016/j.rser.2020.109704.

Darwish, Z.A., Kazem, H.A., Sopian, K., Al-Goul, M.A., Alawadhi, H., 2015. Effect of dust pollutant type on photovoltaic performance. Renew. Sustain. Energy Rev. 41 (2015), 735–744. https://doi.org/10.1016/j.rser.2014.08.068.

EL-Shobokshy, M.S., Hussein, F.M., 1993. Effect of dust with different physical properties on the performance of photovoltaic cells. Sol. Energy 5 (6), 505–511.
Figgis, B., Ennaouia, A., Ahzia, S., Rémond, Y., 2017. Review of PV soiling particle mechanics in desert environments. Renew. Sustain. Energy Rev. 76 (2017), 872–881. https://doi.org/10.1016/j.rser.2017.03.100.
Gholami, A., Saboonchi, A., Alemrajabi, A.A., 2017. Experimental study of factors affecting dust accumulation and their effects on the transmission coefficient of glass for solar applications. Renewable Energy 112 (2017), 466–473. https://doi.org/10.1016/j.renene.2017.05.050.
Goossens, D., Van Kerschaever, E., 1999. Aeolian dust deposition on photovoltaic solar cells: the effects of wind velocity and airborne dust concentration on cell performance. Sol. Energy 66 (4), 277–289.
Gupta, V., Sharma, M., Pachauri, R.K., Babu, K.N.D., 2019. A comprehensive review of the effect of dust on the solar photovoltaic system and mitigation techniques. Sol. Energy 191 (2019), 596–622. https://doi.org/10.1016/j.solener.2019.08.079.
Hachicha, A.A., Al-Sawafta, I., Said, Z., 2019. Impact of dust on the performance of solar photovoltaic (PV) systems under United Arab Emirates weather conditions. Renewable Energy 141, 287–297.
Hammad, B., Al–Abed, M., Al–Ghandoor, A., Al–Sardeahe, A, and Al–Bashir, A., 2018. Modelling and analysis of dust and temperature effects on photovoltaic systems' performance and optimal cleaning frequency: Jordan case study. Renew. Sustain. Energy Rev., 82 (2018), 2218–2234. doi: http://dx.doi.org/10.1016/j.rser.2017.08.070.
Hassan, G., Yilbas, B.S., Said, S.A.M., Matin, A., 2016. Chemo-mechanical characteristics of mud formed from environmental dust particles in humid ambient air. (22 July 2016 ed., Vol. 6). Natl. Res.: Sci. Rep.
Ilse, K.K., Figgis, B.W., Naumann, V., Hagendorf, C., Bagdahn, J., 2018. Fundamentals of soiling processes on photovoltaic modules. Renew. Sustain. Energy Rev. 98 (2018), 239–254. https://doi.org/10.1016/j.rser.2018.09.015.
Isaifan, R.J., Johnson, D., Ackermann, L., Figgis, B., Ayoub, M., 2019. Evaluation of the adhesion forces between dust particles and photovoltaic module surfaces. Sol. Energy Mater. Sol. Cells 191, 413–421.
Jiang, Y., Lu, L., Ferro, A.R., Ahmadi, G., 2018. Analyzing wind cleaning process on the accumulated dust on solar photovoltaic (PV) modules on flat surfaces. Solar Energy 159, 1031–1036. https://doi.org/10.1016/j.solener.2017.08.083.
Jiang, Y., Lu, L., Sun, K., 2011. Experimental investigation of the impact of airborne dust deposition on the performance of solar photovoltaic (PV) modules. Atmos. Environ. 45 (2011), 4299–4304. https://doi.org/10.1016/j.atmosenv.2011.04.084.
Kalashnikov, O.V., Sokolik, I.N., 2004. Modelling the radiative properties of non-spherical soil-derived mineral aerosols. J. Quant. Spectrosc. Radiat. Transfer 87 (2004), 137–166. https://doi.org/10.1016/j.jqsrt.2003.12.026.
Kaldellis, J.K., Kapsali, M., 2011. Simulating the dust effect on the energy performance of photovoltaic generators based on experimental measurements. Energy 36 (2011), 5154e5161. https://doi.org/10.1016/j.energy.2011.06.018.
Kaldellis, J.K., Fragos, P., Kapsali, M., 2011. Systematic experimental study of the pollution deposition impact on the energy yield of photovoltaic installations. Renew. Energy 36 (2011), 2717–2724. https://doi.org/10.1016/j.renene.2011.03.004.
Kalogirou, S., 2009. Solar Energy Engineering: Processes and Systems. Academic Press, Elsevier, London.
Kazem, H.A., Chaichan, M.T., 2019. The effect of dust accumulation and cleaning methods on PV panels' outcomes based on an experimental study of six locations in Northern Oman. Solar Energy 187 (2019), 30–38. https://doi.org/10.1016/j.solener.2019.05.036.
Kazem, H.A., Khatib, T., Sopian, K., Buttinger, F., Elmenreich, W., Albusaidi, A.S., 2013. Effect of dust deposition on the performance of multi-crystalline photovoltaic modules based on experimental measurements. Int. J. Renew. Energy Res. 3 (4), 850–853.
Kalogirou A, S, Agathokleous, R, Panayiotou, G, 2013. On-site PV characterization and the effect of soiling on their performance. Energy 51 (1), 439–446. https://doi.org/10.1016/j.energy.2012.12.018.
Kazem, H.A., Chaichan, M.T., 2016. Experimental analysis of the effect of dust's physical properties on photovoltaic modules in Northern Oman. Sol. Energy 139 (2016), 68–80. https://doi.org/10.1016/j.solener.2016.09.019.
Kazmerski, L.L., Diniz, A.S., Maia, C.B., Viana, M.M., Costa, S.C., Brito, P.P., Campus, C.D., Neto, V.L.M., Hanriot, S., Oliveira Cruz, L.R., 2016. Fundamental studies of adhesion of dust to pv module surfaces: chemical and physical relationships at the microscale. IEEE J. Photovoltaics 6 (3), 719–729. https://doi.org/10.1109/JPHOTOV.2016.2528409.
Klugmann-Radziemska, E., 2015. Degradation of the electrical performance of a crystalline photovoltaic module due to dust deposition in northern Poland. Renew. Energy 78 (2015), 418–426. https://doi.org/10.1016/j.renene.2015.01.018.
Li, C., Kattawara, G.W., Yang, P., 2004. Effects of surface roughness on light scattering by small particles. J. Quant. Spectrosc. Radiat. Transfer 89 (2004), 123–131. https://doi.org/10.1016/j.jqsrt.2004.05.016.
Mani, M., Pillai, R., 2010. Impact of dust on solar photovoltaic (PV) performance: Research status, challenges and recommendations. Renew. Sustain. Energy Rev. 14 (2010), 3124–3131. https://doi.org/10.1016/j.rser.2010.07.065.
Mishra, S.K., Agnihotri, R., Yadav, P.K., Singh, S., Prasad, M.V.S.N., Praveen, P.S., Tawale, J.S., Rashmi, Mishra, N.D., Arya, B.C., Sharm, C., 2015. Morphology of atmospheric particles over semi-arid region (Jaipur, Rajasthan) of India: implications for optical properties. Aerosol Air Quality Res. 15, 974–984.
Nahar, N.M., Gupta, J.P., 1990. Effect of dust on transmittance of glazing materials for solar collectors under arid zone conditions of India. Solar & Wind Technol. 7 (2–3), 237–243. https://doi.org/10.1016/0741-983X(90)90092-G.
Nirmal, A., Kyaw, A.K.K., Sun, X.W., Demir, H.V., 2014. Microstructured porous ZnO thin film for increased light scattering and improved efficiency in inverted organic photovoltaics. Opt. Express 22 (S6), A1412–A1421. https://doi.org/10.1364/OE.22.0A1412.
Picotti, G., Borghesani, P., Cholette, M.E., Manzolini, G., 2018. Soiling of solar collectors – Modelling approaches for airborne dust and its interactions with surfaces. Renew. Sustain. Energy Rev. 81 (2018), 2343–2357. https://doi.org/10.1016/j.rser.2017.06.043.
Potenza, M.A.C., Albani, S., Delmonte, B., Villa, S., Sanvito, T., Paroli, B., Pullia, A., Baccolo, G., Mahowald, N., Maggi, V., 2016. Shape and size constraints on dust optical properties from the Dome CICE core, Antarctica (16 June 2016 ed., Vol. 6:28162). Sci. Rep.
Qasem, H., Betts, T.R., Mullejans, H., AlBusairi, H., Gottschalg, R., 2011. Effect of dust shading on photovoltaic modules. In: Paper presented at the Proceedings of the 26th European Photovoltaic Solar Energy Conference and Exhibition (26th EUPVSEC) Hamburg, Germany.
Said, S.A.M., Walwil, H.M., 2014. Fundamental studies on dust fouling effects on PV module performance. Sol. Energy 107 (2014), 328–337. https://doi.org/10.1016/j.solener.2014.05.048.
Sarver, T., Al-Qaraghuli, A., Kazmerski, L.L., 2013. A comprehensive review of the impact of dust on the use of solar energy: History, investigations, results, literature, and mitigation approaches. Renew. Sustain. Energy Rev. 22 (2013), 698–733.
Sayyah, A., Horenstein, M.N., Mazumder, M.K., 2014. Energy yield loss caused by dust deposition on photovoltaic panels. Sol. Energy 107 (2014), 576–604. https://doi.org/10.1016/j.solener.2014.05.030.
Sisodia, A.K., Mathur, R.M., 2019. Impact of bird dropping deposition on solar photovoltaic module performance: a systematic study in Western Rajasthan. Environ. Sci. Pollut. Res. 26 (30), 31119–31132. https://doi.org/10.1007/s11356-019-06100-2.
Sulaiman, S.A., Hussain, H.H., Nik Leh, N.S.H., Razali, M.S.I., 2011. Effects of dust on the performance of PV panels. Int. J. Mech. Mechatron. Eng. 5 (10), 2028–2033 scholar.waset.org/1307-6892/10305.
Tanesab, J., Parlevliet, D., Whale, J., Urmee, T., 2019. The effect of dust with different morphologies on the performance degradation of photovoltaic modules. Sustainable Energy Technol. Assess. 31 (2019), 347–354. https://doi.org/10.1016/j.seta.2018.12.024.
Tanesab, J., Parlevliet, D., Whale, J., Urmee, T., Pryor, T., 2015. The contribution of dust to performance degradation of PV modules in a temperate climate zone. Sol. Energy 120 (2015), 147–157. https://doi.org/10.1016/j.solener.2015.06.052.
Taylor, H.F.W., 1992. Cement Chemistry. Academic Press Inc, London.
Wang, H., Meng, X., Chen, J., 2020a. Effect of air quality and dust deposition on power generation performance of the photovoltaic module on the building roof. Build. Service, Eng., Res. Technol. 41 (1), 73–85. https://doi.org/10.1177/0143624419868806.
Wang, P., Kong, M., Du, W., Wang, L., Ni, L., 2020b. The effect of pollutants on leakage current and power degradation of photovoltaic modules. Renew. Energy 146 (2020), 2668–2675. https://doi.org/10.1016/j.renene.2019.08.055.
Zaihidee, F.M., Mekhilef, S., Seyedmahmoudian, M., Horan, B., 2016. Dust as an unalterable deteriorative factor affecting PV panel's efficiency: Why and how. Renew. Sustain. Energy Rev. 65 (2016), 1267–1278. https://doi.org/10.1016/j.rser.2016.06.068.